T.R.
BOLU ABANT İZZET BAYSAL UNIVERSITY
INSTITUTE OF GRADUATE STUDIES
DEPARTMENT OF CHEMICAL ENGINEERING

Improvement of the Desalting Process For Crude Oil by Field Validated-Flowsheet Simulation

MASTER OF SCIENCE

HARETH ABBAS FARAJ

ACADEMIC SUPERVISOR
Prof. Dr. Turgay Pekdemir

BOLU, JULY-2024

APPROVAL OF THE THESIS

Improvement of the Desalting Process For Crude Oil by Field Validated-Flowsheet Simulation submitted by **Hareth Abbas Faraj** and defended before the Examining Committee Members listed below in partial fulfillment of the requirements for the degree of **Master of Science** in**, Chemical Engineering, Institute of Graduate Studies of Bolu Abant Izzet Baysal University in 3.07.2024** by

Examining Committee Members	**Signature**
Supervisor Prof. Dr. Turgay Pekdemir Bolu Abant Izzet Bayasal University	.....
Member Assoc. Prof. Dr. Güler Bengüsu Tezel Bolu Abant Izzet Bayasal University	.....
Member Prof. Dr. Barış Şimşek Çankırı Karatekin University	.....

Prof. Dr. İbrahim KÜRTÜL
Director of Instıtute of Graduate Studies

ETHICAL DECLARATION

In this thesis dissertation that was properly prepared according to the Thesis Writing Rules of Bolu Abant İzzet Baysal University of the Institute of Graduates Studies, I hereby declare that;

- All data, information, and documents presented in the thesis were obtained in accordance with the academic and ethical rules,
- All data, documents, assessments, and results were presented in accordance with the scientific ethical and moral rules,
- All works that were benefitted in the thesis were appropriately cited,
- No alteration was made in the data used,
- Study presented in this thesis is original,

Otherwise, I declare that I accept the loss of all my rights in case any contradiction that may arise against me.

The similarity rate obtained by using the Turnitin program, a plagiarism detection software, is within the limits approved by University Senate.

_____

Hareth Abbas Faraj

ABSTRACT

IMPROVEMENT OF THE DESALTING PROCESS FOR CRUDE OIL BY FIELD VALIDATED-FLOWSHEET SIMULATION
MSC THESIS
HARETH ABBAS FARAJ
BOLU ABANT IZZET BAYSAL UNIVERSITY
INSTITUTE OF GRADUATE STUDIES
DEPARTMENT OF CHEMICAL ENGINEERING
SUPERVISOR: PROF. DR. TURGAY PEKDEMIR
BOLU, JULY 2024
(xiii + 85)

When crude oil is extracted from reservoirs, it's common to find water, sediments, and mineral salts. The oil's high salinity is the primary factor contributing to corrosion in pipelines and equipment; it hinders the mass transfer process in the distillation unit's fractionator trays and diminishes the effectiveness of separation, necessitating additional equipment and power. Presently, prevailing requirements for desalted crude oil demand that salt concentrations be below 20 ppm. Thus, treatment in production oil fields is the first line of defense against the effects of salts.

This study aims to improve crude oil desalting by using a verified flowsheet simulation with the most effective set of conditions for crude oil trains. We validated the simulation by comparing it with real field samples in three aspects: composition, dehydrator and desalter efficiency, and process parameters.

The current operating parameters of the selected crude oil train are as follows: temperature, pressure, wash water flow rate, crude oil feed, and demulsifier dosage as 50 °C, 41.5 barg, 21 m^3, 116834 bbl/day, and 29 ppm, respectively. We studied the factors that affect desalting crude oil using case studies by simulation models developed using a commercially available Aspen HYSYS flowsheet simulation software package. The results predicted that in terms of desalting performance, the best operating conditions for treating crude oil were (temperature = 80 °C, pressure = 14 barg, wash water flow = 16 m^3, crude feed = 116834 bbl/day, and demulsifier dosage = 16 ppm).

The results from the simulations showed that the usage of wash water and chemical demulsifier could be significantly reduced while maintaining the targeted crude oil quality: 24% and 45% reduction in wash water flowrate and demulsifier dosage, respectively. Ultimately, the simulated model indicated that the desalting process could significantly improve desalting performance to 3 ppm (pounds of salt per thousand barrels of crude oil), with a major economic impact related to saving chemical demulsifiers in the order of (0.004 $/bbl) of produced oil.

KEYWORDS: Crude Oil, Salt Concentration, Flowsheet Simulation, Aspen HYSYS, Desalting Process, Economic Impact.

ÖZET

HAM PETROL TUZ ARINDIRMA İŞLEMININ SAHA DOĞRULANMIŞ AKIŞ ŞEMASI SIMÜLASYONU ILE İYILEŞTIRILMESI
YÜKSEK LİSANS TEZİ
HARETH ABBAS FARAJ
BOLU ABANT İZZET BAYSAL ÜNİVERSİTESİ
LİSANSÜSTÜ EĞİTİM ENSTİTÜSÜ
KİMYA MÜHENDİSLİĞİ BÖLÜMÜ
TEZ DANIŞMANI: PROF. DR. TURGAY PEKDEMİR
BOLU, TEMMUZ - 2024
(xiii + 85)

Ham petrol kuyulardan çıkarıldığında su ve çökeltiler ve mineral tuzlarının içeren katı maddleri içermesi. Petrolün yüksek tuzluluğu, boru hatları ve ekipmanlardaki korozyona katkıda bulunan birincil faktördür; ayrıştırma işlemi ekipmanları performanslarını, örneğin fraksiyonlama tepsilerindeki kütle transfer sürecini, engeller ve ayırma etkinliğini azaltarak ek ekipman ve güç gerektirir. Günümüzde tuzdan arındırılmış ham petrole yönelik geçerli gereksinimler, tuz konsantrasyonlarının 20 ppm'nin altında olmasını gerektirmektedir. Bu nedenle petrol sahalarında arıtma işlemleri tuzların etkilerine karşı ilk savunma hattıdır.

Bu çalışma, ham petrol işleme tesisi için en etkili koşullarıyla doğrulanmış bir süreç simülasyonu kullanarak ham petrolün tuzdan arındırılmasını iyileştirmeyi amaçlamaktadır. Simülasyonu gerçek saha örnekleriyle üç açıdan karşılaştırarak doğruladık: kompozisyon, kurutucu ve tuz giderici verimliliği ve proses parametreleri.

Seçilen ham petrol treninin mevcut çalışma parametreleri aşağıdaki gibidir: sıcaklık, basınç, yıkama suyu debisi, ham petrol beslemesi ve emülsifiye edici dozajı 50 °C, 41,5 barg, 21 m^3, 116834 varil/gün ve 29 ppm. Ticari bir simülasyon yazılım paketi olan Aspen HYSYS platformunda geliştirilen simülasyon modelleri ile vaka çalışmaları kullanarak ham petrolün tuzdan arındırılmasını etkileyen faktörleri inceledik.

Sonuçlar, tuz giderme performansı açısından ham petrolün arıtılması için en iyi çalışma koşullarının şu şekilde olduğunu gösterdi: sıcaklık = 80 °C, basınç = 14 barg, yıkama suyu akışı = 16 m^3, ham besleme = 116834 varil/gün, ve emülsifiye edici dozaj = 16 ppm. Simülasyonlar, hedeflenen ham petrol kalitesini elde etmenin yanında, yıkama suyu gereksinimini 24% ve kimyasal emülsiyon önleyici kullanımının 45% azaltılabileceğinide gösterdi. Sonuçta simüle edilen model, tuzdan arındırma işleminin, tuzdan arındırma performansını önemli ölçüde 3 ppm'ye (bin varil ham petrol başına pound tuz) kadar artırabileceğini ve kimyasal emülsifiye edicilerden tasarrufla ilgili büyük bir ekonomik etkinin (0.004 $/varil) olabileceğini gösterdi.

ANAHTAR KELİMELER: Ham Petrol, Tuz Konsantrasyonu, Akış Şeması Simülasyonu, Aspen HYSYS, Tuzdan Arındırma Prosesi, Ekonomik Etki.

TABLE OF CONTENTS

LIST OF FIGURES

Page

LIST OF TABLES

Page

LIST OF ABBREVIATIONS AND SYMBOLS

PTB : Pounds of salt per Thousand Barrels of crude oil

GOSP : Gas-Oil Separation Plant

BS&W : Basic Sediments and Water

API : American Petroleum Institute

TAN : Total Acid Number

OPEC : Organization of the Petroleum Exporting Countries

PFD : Process Flow Diagram

LP : Low Pressure

HP : High Pressure

PPM : Parts Per Million

SRE : Salt Removal Efficiency

W/O : Water-in-Oil Emulsion

O/W : Oil-in-Water Emulsion

AC : Alternate Current

DC : Direct Current

DL : Double Layer

WS% : water separation efficiency

W/C : Water Cut

bbl/day : barrels per day

MMSCFH : Million Standard Cubic Feet per Hour

BOC : Basra Oil Company

GC : Gas Chromatography

SimDist : Simulated Distillation

HTGC : High-temperature gas chromatography

ASTM : American Society for Testing and Materials

EPT-# : Chemical Demulsifier Name

PID-# : Chemical Demulsifier Code

C(x)* : Lumped Crude Oil Hydercarbon Components

SCF : Standard Cubic Feet

PR : Peng-Robinson

RVP : Reid Vapor Pressure

PDV : Pressure Differential Valve

FV	**:** Flow Valve
barg	**:** unit of gauge pressure
P	**:** Pressure
T	**:** Temperature
TVP	**:** True Vapor Pressure
R^2	**:** Coefficient of Determination
GOR	**:** Gas-Oil Ratio
B_O	**:** oil formation volume factor
$/bbl	**:** United States dollar per barrel

ACKNOWLEDGMENT

First and foremost, I praise **Allah** almighty, my creator, for giving me all this strength to proceed with faith and perseverance, which sustained me through all the difficulties throughout this long journey of study.

I'm deeply indebted to this work in memory of **my father and mother**, who taught me how to be a man who respects life. I'm eternally grateful to **my brother and his family** for supporting me with love and care. Also, a special thanks to **my sister**; no words can express my feelings towards you. To **my fiancée**, thank you for being the light in my life.

I would like to express my deepest appreciation and gratitude to my supervisor, Prof. Dr. **Turgay Pekdemir**, for supporting me patiently with his time, knowledge, and guidance. I believe that our relationship extends beyond that of a student and supervisor and is characterized as a friendship. Thank you for allowing me to work under your supervision all this time. Also, a special thanks to the **examining committee** members for their efforts and patience.

Lastly, I'd like to extend my sincere thanks to **my teachers** in the past and present, **my close friends**, and **everyone** who supported me.

Hareth

2024

1. INTRODUCTION

Both production oil fields and refineries deal with crude oil, and treatment operations and processes in a gas-oil separation plant (GOSP) to remove water and salt are the first line of defense against salt related problems, which are considered the first enemy for equipment, pipelines, and the price of exported oil. Therefore, it has become necessary that treatment in GOSP be at a high level of efficiency that is commensurate with the global required level (exported barrel price) on the one hand and the local use of oil sent to refineries on the other hand. Field operators are working to improve the efficiency of the desalting process while keeping per-barrel production costs low. It's possible to determine how much value the desalting processes add to the facility as a whole (feasibility) by closely monitoring their effectiveness and cost. From all the literature reviewed in the next chapter, it's clear that the key impact parameters of operating a crude oil desalting train (crude oil composition, temperature, chemical demulsifier dosage, wash water ratio, pH value, mixing degree, electrical treatment, and residence time of crude oil) work together interactively (1,2).

1.1 Aim and Scope of the Study

The aim of the present study is to find the best combination of crude oil train parameters that affect the desalting process based on real field data (Iraqi crude oil samples) that were collected from a plant in one of the Basra oil fields in the south of Iraq by flowsheet simulation modeling. Aspen HYSYS was used to build a flowsheet simulation of a crude oil train based on lab test data on oil samples and the operation conditions of a field-validated flow-sheet.

The main influential parameters on the crude oil desalting train performance, like temperature, pressure, wash water ratio, crude oil feed flow, and demulsifier dosage, were analyzed by case studies of the Aspen HYSYS simulation. The best degree of separation within the ranges of parameters investigated leads to an improved model of crude oil trains, which has a key impact on the process of desalting, consequently leading to an overall economic impact.

1.2 Structure of the Study

- Chapter 1: provides an overview of research within its general framework.
- Chapter 2: provides an in-depth critical review of the literature related to the research subject matter.

- Chapter 3: provides a comprehensive explanation of the methodology employed in the process of collecting and analyzing data from crude oil samples to build a predictive flow sheet simulation by Aspen HYSYS.
- Chapter 4: presents an analysis and discussion of the results obtained from this research.
- Chapter 5: summarizes this research by presenting a comprehensive conclusion and offering suggestions for potential future research projects.

1.3 Crude Oil Separation Overview

Crude oil is extracted from reservoirs by either natural flow or artificial lift systems. The latter, often necessitate the injection of water to sustain reservoir pressure and ensure it remains above saturation pressure. The crude oil is collected from various wells across the field by individual flow lines, covering distances of 1 to 5 kilometers. These flow lines are connected to either local manifolds or remote manifolds, which serve as intermediate collection points. From these manifolds, the crude oil is then transported via trunklines to the treatment facility named as gas-oil separation plant (GOSP).

Firstly, crude oil is processed by separating the oil phase, the gas phase, and the water phase into their own individual streams. This takes place in a two- or three-phase separator, depending on the water content of the stream. This separation is considered as the spine process of gas-oil separation in a chain of field processing units for oil and gas operations.

Secondly, the gas associated with the generated crude causes an increase in pressure, and the separators are employed to relieve this pressure. Another duty of separators is to remove free water from the produced stream when present. Once the streams of various fluid have been separated, they can be processed individually for use in their respective fields.

Water, primarily in the form of emulsion, may make up anywhere from 10% to 15% of oil's total volume. The salty water content of crude oil is a major cause of corrosion and scaling in transportation and refining equipment, leading to the deterioration of these facilities (3). This water content is referred to as basic sediments and water (BS&W) of which water level can be as low as 0.5% but no higher than 1%, with a salty content of no more than 15 PTB (pounds of salt per thousand barrels of crude oil) (4). When the outlet oil from the separator does not

meet the world standards of the oil market, this may require additional processing like de-emulsion techniques and desalting treatment.

1.4 Crude Oil Composition

The term "crude oil" refers to a complex mixture of hydrocarbon compounds that look and smell and have composition different from one field to another. It's founded in a wide range of forms and colours, having components changing from water to tar-like solids, and they can be transparent or black. The molecular range can also vary from C_1 to C_{80} or even further, which, as shown in **Figure 1.1**, are classified under one of the following branches (4,5):

1. Alkanes or Paraffins.
2. Cycloalkanes or Cycloparaffins (Naphthene).
3. Alkenes or Olefins.
4. Aromatics.

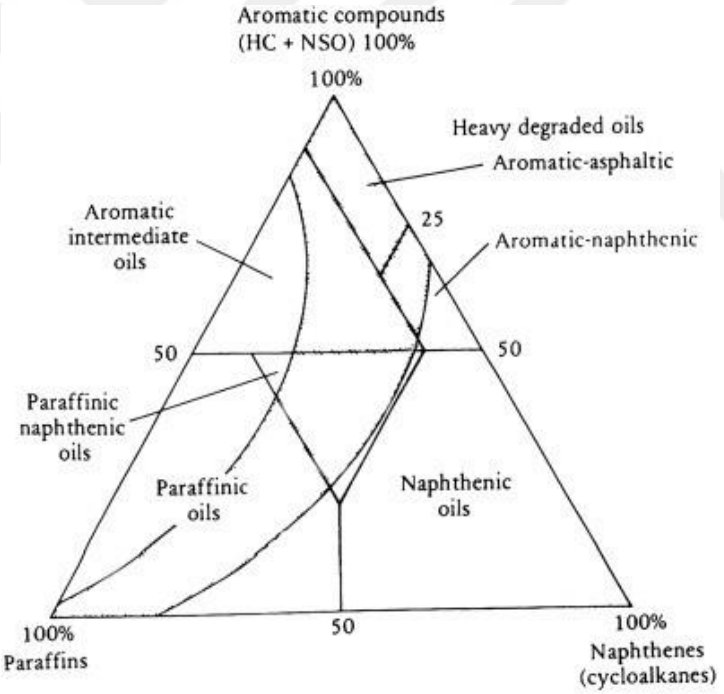

Figure 1.1 Relative percentage of crude oil components (6).

Typical crude oil comprises approximately (82.2% to 87.1%) carbon, (11.7% to 14.7%) hydrogen, (0.1% to 5.5%) sulfur, (0.1% to 1.5%) nitrogen, (0.1% to 4.5%) oxygen (7), and some trace components like nickel and vanadium metallic compounds (8).

1.5 Crude Oil Quality

Generally, crude oil differs from one another by three main primary quality parameters:

1. API gravity

According to the American Petroleum Institute (API), gravity is another way of saying "heavy or light" oils; crude with a higher API number usually has a lot of paraffin and makes more gasoline and other light petroleum products than crude with a lower API number as shown in equation below:

$$\text{API} = \frac{141.5}{\gamma} - 131.5 \quad (1)$$

Where (γ) is the oil specific gravity at 15.5 °C (60 °F).

2. Total acid number (TAN)

TAN is a measure of potential corrosivity; it is the milligram amount of potassium hydroxide (KOH) required to neutralize 1 gram of crude oil. **Figure 1.2** demonstrates that if the TAN number is large, there must be stronger metallurgy than usual to ensure that the processing equipment can withstand the corrosivity.

Figure 1.2 Crude oil corrosivity according to TAN count (9).

3. Sulfur content

Crude oil is called "sour" when it has a lot of hydrogen sulfide or other sulfur components, while it's called "sweet" due to its lower sulfur content. The variation between sour and sweet oils is typically between 0.5 wt % and 1.5 wt % of sulfur, with a split range around 0.5% (10) as shown in **Figure 1.3**.

Figure 1.3 Crude oil sweetness according to sulfur content (9).

Based on the above features of crude oil, the ideal crude oil is light (higher API), sweet (low sulfur content), and has a low TAN count as the oil of North Sea-Brent, Malaysia-Tapis, United States-WTI, and Libya-Light. While the more complicated oil to process is heavy, sour, and has a high TAN count as the oil of Maya from Mexico and OPEC. Both above-mentioned oils and other intermediate oils between them are shown in **Figure 1.4** and **Figure 1.5**.

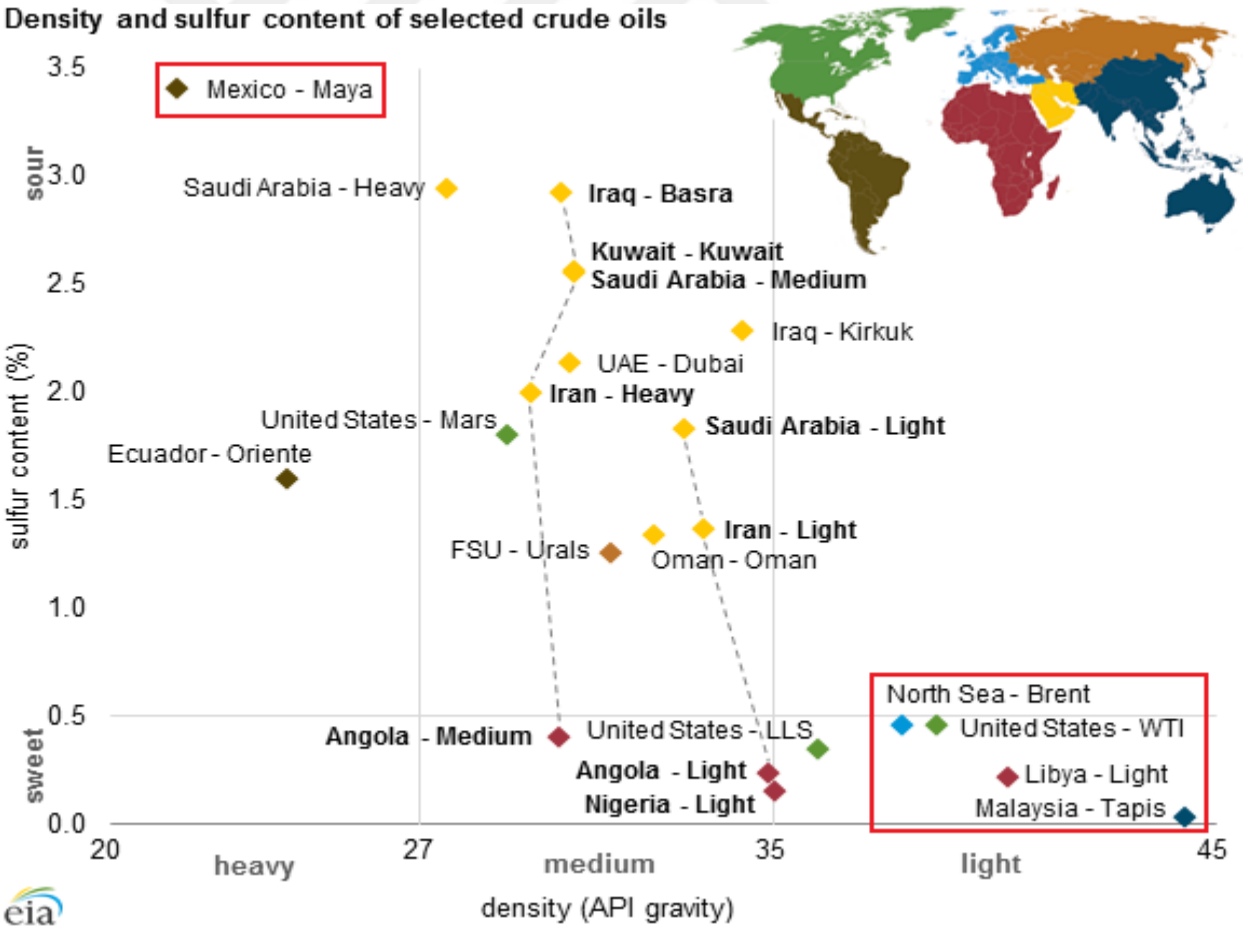

Figure 1.4 Crude oil classification according to its features around the world (11).

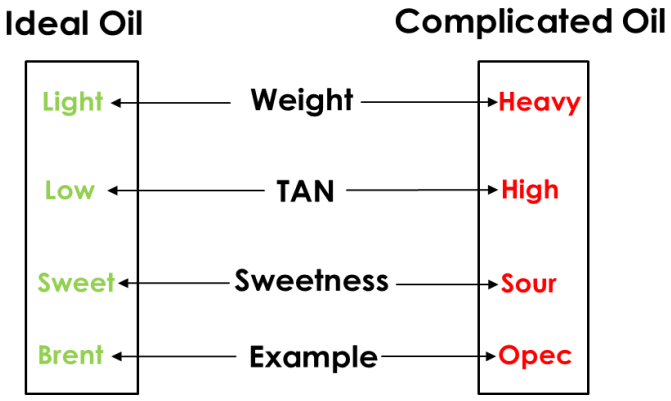

Figure 1.5 Ideal crude oil versus complicated ones.

1.6 Wet Oil

Wet oil is a mixture of water and oil. A breakdown of the oil phase can result from the application of hydrostatic pressure by water to oil within a subsurface reservoir. The water displaces the oil and facilitates its extraction to the surface. Emulsions are formed due to the turbulent flow of crude oil and water during this extraction process. In the late stages of oil well life, nearly all wells generate a greater volume of water in conjunction with their oil output, surpassing the acceptable threshold for business feasibility. The commencement of water production from wells can occur either at the inception of production or after a considerable period of time. Late-stage wells have, thus, the potential to yield either wet oil or dry oil, depending on the drilling technology employed during the first stages. There are various factors that can contribute to the presence of wet oil in wells, such as abrupt and irregular water intrusion, connection between tubing and casing, proximity of casing holes to water layers, fractures or splits between oil and water layers, corrosion-induced casing failure, and inadequate cementing leading to channelling.

Figure 1.6 demonstrates that the failure of the casing is due to either corrosion or subpar cement work, which allows salty water from an above-layer location to enter the well and interfere with oil production. Increased water intrusion could have resulted from further technical reasons. One example is the use of steam or water for injection into the oil reservoir for enhanced oil recovery (EOR). These injection processes aid in or improve the recovery of oil from low-pressure reservoirs. Wet oil is consequently created when water or steam injected into an oil well and combines with the oil. It is more likely that these elements will play a role

in the latter stages of the oil recovery process. Due to the transportation of water in oil emulsions, such as the mixing of formation brine with crude oil, mixing intensifiers have an impact on some desalination and dehydration plants. Perforations in the casing, production tubing, underground safety valves, bottom and wellhead chokes, and limits on flow lines and pipelines all increase the agitation influence. The aforementioned variables primarily determine wet crude output.

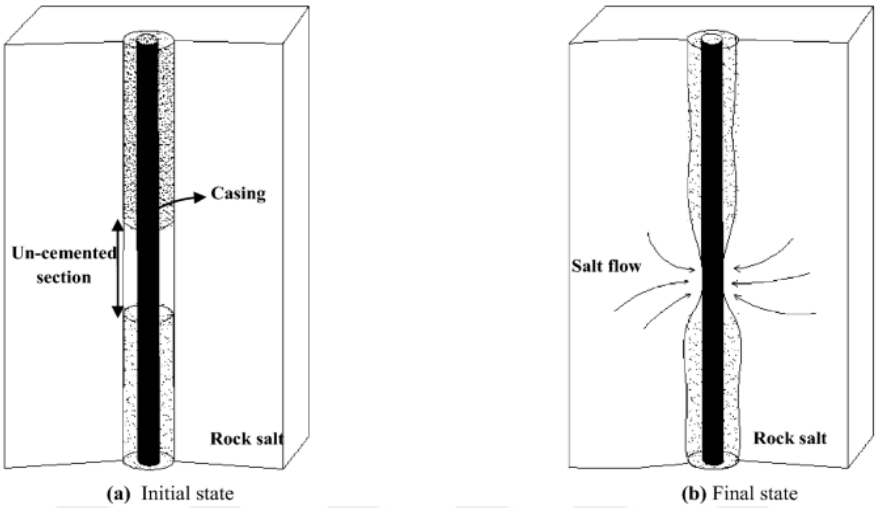

Figure 1.6 Casing failure mechanism shown as: (a) initial state when there is an un-cemented length of casing through salt layer; (b) final state when un-cemented length is filled due to salty water flow (12).

1.6.1 Corrosion Effect

The first priority of the company is to protect the pipelines and equipment from fouling, plugging, and corrosion, as well as to keep the catalysts in the processing units from being poisoned. These crude pollutants must be removed by the processes of desalting and dehydration (3,10,13).

When processing and transporting sour and heavy crudes, corrosion in pipelines and equipment is likely to be severe due to the increase of corrosive compounds like naphthenic acid, sulfides, and mineral salts in crude oil. Therefore, removing all these corrosive causes (salts) is a high priority through a process called dehydration and desalting. Removing the salts from oil is essential as they cause hydrolysis and form hydrochloric acid (HCl), which is the leading cause of corrosion. Below are the equations for salt hydrolysis:

$$MgCl_2 + 2H_2O \rightarrow Mg(OH)_2 + 2HCl \quad (2)$$

$$CaCl_2 + 2H_2O \rightarrow Ca(OH)_2 + 2HCl \quad (3)$$

$$NaCl + H_2O \rightarrow NaOH + HCl \quad (4)$$

Equation of corrosion:

$$2HCl + Fe \rightarrow Fe^{+2} + 2Cl^{-} + H_2 \quad (5)$$

Presence of H_2S:

$$H_2S + Fe \rightarrow FeS + H_2 \quad (6)$$

$$2HCl + FeS \rightarrow Fe^{+2} + 2Cl^{-} + H_2S \quad (7)$$

Reproducing H_2S by reaction of equation 7 keeps reaction of equation 6 continuously feeding with hydrogen sulfide, which leads to unstoppable corrosion (14,15). **Figure 1.7** shows an example of the bad effect of corrosion.

Figure 1.7 Corrosion and scale effect (16).

1.7 Desalting Parameters

Stoke's Law physically governs the separation of water from oil (17–21). To make the water droplets more likely to merge, alternate electricity (sometimes a dual system) creates a dipolar electrostatic force on the droplets of water. Depending on the crude oil's composition and physical properties, it can behave very differently in a desalter. The desalting system can be challenging due to constantly changing process factors. On the one hand, the crude must meet strict quality norms; on the other hand, the under-carry must not be so intense that it impairs the system's ability to dehydrate or contaminate downstream wastewater treatment. Improving the desalting process in a dynamic environment is critical for the overall process operation.

There is a real need to comprehend the desalting operation and its crucial key parameters like the injected demulsifier, temperature of crude, wash water rate, mixing degree, pH of associated water, electrical treatment, and residence time of crude oil because laboratory and field experiments have shown the complexity of the desalting process parameters.

1.7.1 Chemical Demulsifier

A demulsifier is a chemical that facilitates separation of the two phases of an emulsion. Selection and performance evaluation of demulsifiers are typically based on the bottle tests, which are the most typical and widely acknowledged technique in the crude oil industry. The method is dependent upon a visual inspection of emulsion phase separation in normal-graded bottles. In addition to visual inspection, analysis is based on the rapidity of phase separation. It is a time-consuming, hands-on method that requires a skilled engineer to interpret the results and choose an efficient dosage of demulsifier (22).

Demulsifiers are a type of chemical compound that is composed of several components that each have their own unique molecular structure and molecular weight allocation. The numerous constituents of a demulsifier need to each have their own unique capability for dividing as well as their own unique interfacial activity. The ability to change boundary rheological properties, such as by lowering the interface stickiness and raising the compressibility, in order to encourage film drainage and the narrowing of the lamellae between the droplets has the ability to destabilize the protective layer coating the droplet of water by possessing a great attraction to the interface of the emulsion. All these above are the most important destabilizing features of a good demulsifier (23–25).

Water- and oil-based demulsifiers produce varying degrees of water separation depending on demulsifier dose, residual time of crude oil, and demulsifier characteristics like pH.

Yazdanmehr and her co-worker show that the demulsifier pH has a 27% effect on dehydration efficiency, while other factors such as dosage as well as residence duration have much smaller effects. She shows that the best results can be achieved by using a water-based demulsifier with the following parameters: pH =7.76; dosage = 100 ppm; time = 600 minutes; error margin = 10% (26).

Mohammed and his colleagues (25) in the third paper of their series presented a study that involved bottle tests with various demulsifiers on emulsions

of 10% water in Buchan crude oil. The resolution of the emulsion rose with the concentration of a low-to-moderate dosage of demulsifier. They are shown two styles of behavior: the first one, where water separation remained stable with respect to the increase in concentration, and the second one, where water separation decreased as concentration rose. The first behavior resulted from water droplets dissolving and forming a liquid crystalline phase, while the second behavior resulted from growing drops becoming sterically stabilized. The researchers concluded that an overdose of demulsifiers can have the opposite effect, where demulsifiers can clump together in water or oil, making a more viscous phase or helping to stabilize the emulsion by making it less likely to separate.

1.7.2 Temperature

Many crude oil plants (dehydrators and desalters) use heat in the treatment process because it aids in phase separation (coalescence and settling) by decreasing the viscosity of the oil, weakening or rupturing the film between oil and water droplets by expanding the water, and modifying the difference in specific gravity between fluids, thereby reducing settling time. Heat effectively accelerates the treatment process and is most commonly utilized to minimize the size of the treating vessel. However, setting the right temperature throughout the operation of desalting is a sensitive process because any excessive heat could result in the evaporation (the light end) of crude oil. Unless precautions are taken to conserve them, API gravity and volume will fall, which not only leads to a loss of a percentage of oil volume but also decreases the price of a barrel of oil due to a decrease in API gravity. And also, the cost of heating and necessary equipment should be considered. For that, it may be desirable to process crude oil at lower temperatures (27,28).

Additionally, heat reduces the viscosity of the continuous phase (oil), allowing water droplets to move faster and more rapidly towards coalescence. The higher thermal energy of droplets of water helps to spread out (disperse) asphalt aggregates, and more voids make it easier for demulsifiers to get into the oil and stick to the water droplets. These speeds up the rate at which the film thins and drains, which causes more water droplets to coalesce (29).

By lowering the surface tension between oil and water and allowing droplets to combine more easily, heating has an impact on the emulsifier and increases water separation significantly. Reducing the oil's viscosity causes drips to fall faster compared to when the oil's viscosity is higher. It shows that the apparent viscosity

decreases due to the increase in interfacial tension and temperature. The rate of separation in an emulsion also varies with decreasing temperature. Similar to many other chemical processes, temperature accelerates the separation of emulsions. Although there is a discernible influence from temperature, it seems that water content is the main factor influencing emulsion viscosity (30).

The initial temperature of crude oil impacts the aggregation level of asphaltene molecules, whereas a lower initial temperature results in less aggregation and enhanced dispersion of asphaltene. Furthermore, the initial temperature is related to the adsorption rate of crude oil and particles on the interface (31).

In a related context, the effect of heating boosts the crude oil's electrical conductivity. If the conductivity is too high, the voltage difference between the electrodes will be excessive, leading to higher electricity costs and, in the worst-case scenario, short-circuiting and desalter breakdown. While the temperature drops, the settling velocity drops with it, potentially lowering the unit throughput or causing brine carry-over into the crude. Due to the negative nature of both of these outcomes, upper and lower temperature boundaries are typically set for desalter procedures (32).

However, the crude temperature is controlled to avoid evaporation in the electrical desalter and prevent damage to the electrical grid insulator bushings (15).

1.7.3 Wash Water Application

Emulsion salts are typically found in crystalline form. Therefore, desalting techniques require the addition of freshwater to dissolve these crystal salts. To improve "mixing" efficiency and avoid scaling inside pipelines and heating tubes, freshwater is often injected before heat exchangers. "Wash water", also known as "dilution" water, refers to the freshwater used to flush out the water droplets in emulsions before they are drained away. Diluting the high salt content of wet crude by adding less salt water is critical. The wash water's even distribution in crude facilitates the formation of larger droplets, which aids in the acceleration of this separation process. The quantity of wash water injected depends on the API gravity of crude oil, but, generally, the injection rate ranges from 3% to 10% of the overall crude oil flow (28,33).

Water and oil emulsion is produced as a consequence of mixing. Using dehydration techniques, the oil and emulsion are then dehydrated. The separated

water is disposed of by the system for the treatment and disposal of field-produced water. In a two-stage desalting system, dilution water is added to the second stage, and all or a portion of the water discarded in the second stage is recycled and used as dilution water in the first stage. Two-stage desalting plants are normally used to minimize wash water requirements (5).

The salt removal efficiency (SRE) has been found to be improved by increasing the wash water rate up to 6 vol.% of the inlet crude oil (34). This increase in the wash water rate leads to a decrease in the quantity of salt contained in the processed crude oil. Nevertheless, introduction of additional wash water in a proportion beyond the aforementioned percentage does not yield an enhancement in the efficacy of salt removal leads to a decline in performance, this phenomenon occurs due to the direct correlation between the increase in volume of the dispersed phase and the corresponding rise in the specific surface area of the droplets (34).

1.7.4 Mixing Intensity

For efficient desalting, good contact between the crude oil and the washing water is essential. However, the water droplets should not be smaller than the minimum droplet size supported by the settler (35). High shear actions form emulsions. Similarly, when dilution water (freshwater) is added to an emulsion, one needs to mix them in order to dissolve the salt crystals and aid in coalescing finely distributed droplets. Properly selected mixing intensity works in three steps: 1) it helps smaller drops join together; 2) it mixes chemical/demulsifier with the emulsion; and 3) it breaks the free injected volume of wash water into emulsion-sized drops and evenly distributes them (28).

1.7.5 pH (Hydrogen Potential)

Most crude oil emulsions have a preferred pH range; surfactant is usually not needed at all when the film pH is intermediate, or only a little amount is needed to break the emulsion. At moderate pH values, the interfacial tension is only minimally reduced by the surfactants that are naturally present in crude oil. These natural compounds exhibit competitive surfactant properties with commercial surfactants in highly acidic or basic situations (low or high pH). Therefore, commercial surfactants can easily replace natural surfactants at the interface under the intermediate pH (near to 7) values of most produced emulsions (36).

However, from a cost-saving perspective, it is preferable to apply only as much surfactant as is strictly necessary to achieve the emulsion-breaking time

frame. The interface in the emulsion is often not fully covered by the commercial surfactant used under these conditions. This creates a layer of a combination of natural and commercial surfactants that controls the emulsion's stability. The optimum pH for maximum emulsion instability depends on both the crude oil and brine compositions; brine composition is more important from the standpoint of the economics of pH adjustment (37).

Additionally, pH affects the type of emulsion formed; when low pH near 3 (acidic), surfactants dissolve in the crude oil phase, producing W/O emulsions corresponding to oil-wetting solid films, whereas high pH, more than 11 (basic), causes surfactants to dissolve in the water phase, producing O/W emulsions corresponding to water-wetting mobile soap films (38).

Furthermore, dilution amplifies the difference in density between water droplets and the oil layer, as Elgibaly and his colleague (39) report that the dilution process can be utilized to make the crude phase less viscous, thereby enhancing the desalting and dehydration processes.

In cases of low pH, the interfacial tension between two liquids is the greatest due to asphaltenes, which are resistant in acidic environments, settling into the interfacial layer of an oil-in-water emulsion and increasing its surface tension. High pH causes a greater quantity of water to separate from the emulsion, resulting in an increase in emulsion instability. Therefore, the proportion of water extracted from an emulsion will be lowest in acidic environments and highest in alkaline ones.

Another reason higher pH makes emulsions more stable is because the deposition of OH^- creates a thick surface on the emulsion layer, making it more stable and more difficult to separate. This is due to the fact that alkaline conditions mitigate acidic species, such as naphthenic acids or phenolic compounds, during soap formation. These surfactants, which are generated during the desalting process, frequently increase BS&W values, reduce salt removal, and promote oil/water interface formation, all of which make desalting more difficult. Changing the pH can have an impact on the naphthenic acids in crude oil and, consequently, the stability of water in oil emulsions. However, it appears to be most effective at treating oil-in-water emulsions when the water phase is continuous (1,40).

The hydrophilicity of surfactants is enhanced with an increase in the pH level of the emulsion. So that the formation of asphaltene films is most consistently

observed in an acidic environment. Consequently, elevating the pH level will result in a decrease in the stability of the emulsion (41).

The stability of an emulsion is determined in large part by the kind of crude oil used to make it. As a result, the pH range of 5 to 9 seems to be the tipping point for treating crude oil emulsions (42).

1.7.6 Electrical Treatment

The application of electrostatic coalescence in commercial crude oil environments include the dehydration and desalting. It enables the resolution of water-in-oil emulsions that are relatively stable. Electrical forces are produced by using alternate current (AC) and/or direct current (DC) fields with high voltage. The application of these fields produces electrical forces that enable tiny droplets to coalesce together to the point where sedimentation is governed by gravity.

When a water droplet is suspended in crude oil, it takes on a completely spherical shape if no external forces are acting on it. If a high-voltage field is applied, the droplet will deform into an ellipsoid with opposite charges at both ends. A positive charge within the droplet will sprint to the end of the direction of the negative electrode of the external electric field. In the same way, negative charges in the droplet will sprint to the nearest positive electrode. Two adjacent particles will be electrically attracted to one another during this process. The negative end of one droplet will be close to the positive end of another, producing an attraction force that tends to draw the droplets together. This attraction force can be given by the following equation (43):

$$F = \frac{KE^2 d^6}{S^4} \tag{8}$$

Where:

(F) is the attraction force between droplets,

(K) is the dielectric constant,

(E) is the voltage gradient,

(d) is the diameter of the droplet,

(S) is the distance between the droplets.

From the equation above, it is clear that in order to increase the force of attraction between water droplets and induce them to coalesce, it is necessary to: increase the diameter of water droplets; decrease the distance between droplets; and raise the voltage gradient of the transformer. Once the voltage gradient supplied to

a droplet reaches its critical voltage (Ec), the tiny droplets begin to deform, and their films rupture at the critical point, leading to their breaking up and aggregating into bigger droplets, as shown in **Figure 1.8**.

Below is the mathematical equation of critical voltage (43):

$$E_c = K\sqrt{\frac{T}{d}} \tag{9}$$

Where:

(Ec) is the critical voltage gradient,

(T) is surface tension.

Based on that, when water droplets in oil are exposed to high-voltage alternating electric fields, two significant effects occur: the droplets deform, and the droplets attract one another. Electrophoretic motions are established when unidirectional electric fields are applied; this can increase the frequency of collisions between droplets due to contact charging of droplets upon interaction with the electrodes (44). When the electrical surface charge plays a significant role in determining stability, an O/W emulsion is easier to produce than a W/O emulsion due to the thicker electric double layer in water. This, however, does not mean that W/O emulsions can't be stabilized (45). The majority of particles in aqueous media are charged for a variety of reasons, including the ionization of surface groups, the specific adsorption of ions, etc. The non-uniform distribution of ions surrounding a charged particle in an electrolyte solution gives shape to an electric double layer (DL) (22).

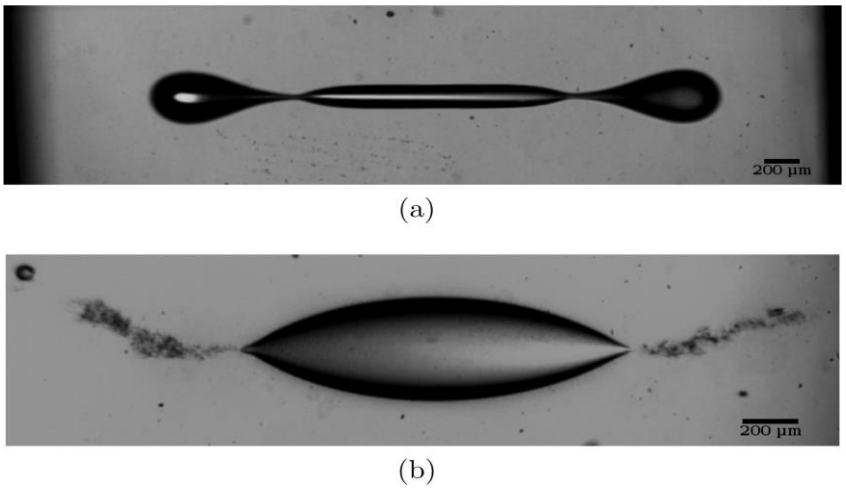

Figure 1.8 Breakup of water droplet suspended in dielectric crude oil under a uniform direct current electric field: (a) lobe formation breakup mode without OTS in the oil; and (b) tip-streaming breakup mode with OTS in the oil (46).

Droplet coalescence could be aided or hindered by the electric field-induced motion of droplets via electrophoresis and dielectrophoretic. There are three stages of processes in droplet coalescence: the initial step is the approach of the droplets, then the drainage of the oil film between the droplets, and ultimately the breaking of the thin film. By creating dipolar pressures between adjacent droplets, an electric field enhances attraction between them (47), as shown in **Figure 1.9**.

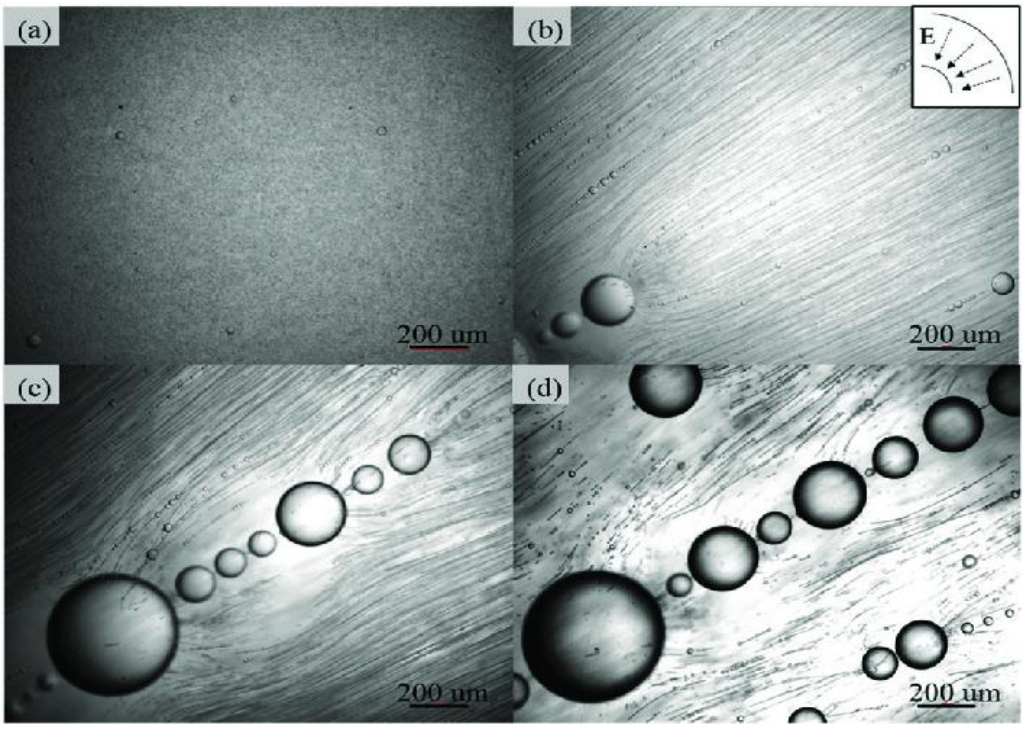

Figure 1.9 Electro coalescence of water-in-oil emulsion (a) t=0 s; (b) t=10 s; (c) t=20 s; (d) t=40 s (48).

1.7.7 Residence Time

Desalters are built to allow for enough settling time (4-5 minutes) during the gravity separation of water (28). The characteristics of the crude and the process variables determine the appropriate residence time. Also, features of crude oil like density, viscosity, water cut, suspended particles, and asphaltene fraction are the primary crude parameters that affect residence time. Formation water in crude oil could be found in two types: free and emulsified. The free water forms bigger drops distributed via the oil phase and is not closely mixed in the crude. Emulsified water, whereas, is tightly combined and distributed in teeny droplets in the oil phase. This type is difficult to remove by simple settling systems, necessitating additional

processing like fresh water, chemical demulsifiers, heating, mixing, and electric field.

Finely dispersed brine droplets (less than 10 microns) in a crude oil emulsion are sufficiently small that the settling velocity due to the density difference between the brine and the oil became unacceptably low (28,49,50). As a useful approximation, one can describe the settling velocity of a brine (V) drop of radius r and density ρw through an oil of density ρo and viscosity μ in terms of Stokes' Law (27):

$$V = Kr^2 \frac{(\rho w - \rho o)}{\mu} \quad (10)$$

Where:

(K) is a suitable constant.

Based on the above equation, it is clear that gravitational separation can be higher based on: increasing the radius of the water droplet (r), increasing the value of the differential densities between water droplets and the oil phase (ρw - ρo), and decreasing the viscosity of the oil phase (μ). By injecting dilution water as well as heating, the difference in densities would increase and the viscosity of the oil would decrease, while using electrical voltage would increase the water droplet's radius. The average residence time of the oil phase decreases as the water level in the vessel increases, but the trend in the water phase is the opposite of that of the oil phase (51).

2. LITERATURE REVIEW

Nowadays, operators working in the oil fields are looking into ways to use novel desalting methods (52–57). These methods are based on improvements to the way processes are designed, and they are being used along with enhancements to oil recovery and how crude oil is moved.

Desalting and dehydration of crude oil are critical for removing undesirable components like salt and water (43,58), before reaching any primary unit operations (59). However, numerous additional impurities must be removed, including clay, silt, rust, and other debris (60). Allowing these substances to deposit on heat transfer surfaces can cause corrosion and fouling, which can harm downstream equipment. Also, the presence of some metals can corrode refining catalysts (61–63).

Maintaining a precise balance between mixing intensity, wash water quality, chemical demulsifier dosage, and other parameters contributing to optimum salt removal is important for process economics and product quality, where improving the desalting process is critical for the overall operation process (64).

This chapter presents a literature review that focuses on the most significant works that have been relevant to desalting simulations in the context of total oil production.

2.1 Crude Oil Demulsification

While oil is extracted from reservoirs, formation water is also removed. Water production from a well is typically modest early in the well's lifecycle but can increase to (95-98) % or more of the total liquid production late in the well's life. Crude oil contains formation water due to primarily geological reasons, as salt water usually rests beneath oil in the strata from which it is extracted (27). As a field's production history grows, more and more formation water pumps into the well and is produced with the oil (6,41,57). Most producing wells will, thus, at some point in their lifetimes, produce water with oil, either because of the formation's initial characteristics or other factors. When water and oil are brought into proximity to one another, emulsification can occur. This can happen naturally in the formations or mechanically in the chokes, pipeline system, separators, and feed pumps where mixing occurs in the presence of surface-active agents (emulsion promoters) in the oil. When the aqueous medium is the dispersed phase, the

combination is referred to as a water-in-oil (W/O) emulsion, and when the oil is the dispersed phase, the mixture is referred to as an oil-in-water (O/W) which sometime might be referred as a reverse emulsion (38,65–67).

Pekdemir et al. (68) clarified that oil and water separated into their respective phases without using a surfactant after being mixed. Over a few days, the contents stirred up again, forming small cellular pockets of water between thin layers of oil that gradually shrank in size. It took a month for them to shrink to the sub-millimeter range. According to their study, oil has a surface-active component that is gradually adsorbed toward the O/W interface. Over time, O/W emulsions with surfactants added to the oil phase remained stable. As the concentration of the surfactant went up, less oil separated at the surface, and the emulsion below the layer of separated oil was of the W/O type. Additionally, as more oil separated at the surface, the amount of the aqueous phase within the mixture increased. They investigated the effect of small solid particles in the produced oil on emulsion stability. The author found that hydrophobic silica formed a coarse emulsion that accounted for around 20% of the overall volume, while hydrophilic silica seemed not to affect stabilizing the emulsion. They conducted additional demulsification tests using a different oil sample, and the results demonstrated that could create stable emulsions without adding surfactants. The authors demonstrated that identifying the oil's background is essential because demulsification and emulsion properties strongly depend on the oil's composition.

The concentration of asphaltenes and resins, as surface active agents, present in the oil is particularly influential in emulsion formation. Density, viscosity, and interfacial tension are other physicochemical parameters that can play a significant role in emulsion formation (69–72).

Meiming He and his colleagues (31) investigated the specific impact of heating on the emulsifying capability of crude oil and its mechanism using tests and molecular simulations. They determined that there was a heating impact during the heating process, which briefly enhanced the emulsifying capability of crude oil. They concluded that a lower initial temperature resulted in reduced aggregation of asphaltene molecules, leading to an enhanced dispersion state of asphaltene, where the lower the initial temperature, the higher the adsorption rate of the crude oil and components on the interface, and the lower the interfacial tension. Moreover, the higher the activity of the components, the stronger the heating impact. At elevated

temperatures, the interfacial strength briefly increased due to the heating impact. Heating can reduce the dissipation of contact forces between asphaltene molecules, leading to an increase in interfacial layer thickness and steric hindrance. This enhances the crude oil's emulsifying ability. At elevated temperatures (80 °C), the interfacial coating became unstable, causing the emulsifying capacity of crude oil to revert to its original state after a certain period.

The increase in the interfacial area between dispersed droplets and the bulk phase means an increase in the free energy of the system. This suggests that mixtures (emulsions) are not thermodynamically stable; consequently, they diminish the interfacial surface area by separating it. For separation to take place, the emulsion droplets have to combine and merge; the phases are then separated by sedimentation (73,74).

2.2 Crude Oil Dehydration

Dhuldhoya and co-workers (75), dealt with dehydration of two kinds of crude oil obtained from Maureen (API 14.6°), an abandoned crude oil field located in the center of the North Sea, on British territory, and Heimdal (API 11.1°), Norway's Petroleum Production. The disc stack centrifuge was able to get them to a quality greater than 0.5% BS&W. The disc stack centrifuge separation method was able to dehydrate both the Maureen and Heimdal crude oils to a higher quality than the specified requirements of the design without the addition of a demulsifier chemical. However, the required operating temperature was 97 °C (207 °F). To enable the centrifuge to dehydrate the oil more rapidly while still meeting or exceeding design specifications, a demulsifier chemical was added. Maureen crude, with its greater API gravity and lower viscosity at treatment temperatures, was somewhat less difficult to dehydrate than Heimdal crude. Using data on water cuts and particle distributions, the centrifuge's performance was calculated with a nominal capacity of 15,000 BPD for processing the crude, but in order to reach 0.5% BS&W with a feedstock of 30% BS&W, the design foundation for processing Maureen crude would need to be down-rated. These analyses aided the process selection and design phases by providing data on which to base decisions. To reach a conclusion, the most effective methods available in the field economy will be used.

Kim and his coworkers (76) built an electrostatic dehydrator. Being used, they demulsified water in oil emulsions constantly by applying a high voltage

alternating current. The levels of demulsification were studied by adjusting some of the factors in the experiment. On an emulsion of the water in oil type, the demulsification process that occurs during oil healing has already been simulated using the intensity of the magnetic field as well as electrical frequency, temperature degree. The water droplets ranged in size from around 15 to 60 millimeters and remained mostly unchanged for about a month when kept at ambient temperature. Both DC and AC fields can be utilized to bring about an effective demulsification process. The particle electrophoresis motion increases the likelihood of coalescence in DC current, even though in AC fields, a larger velocity in the bulk phase is required to achieve the same level of coalescence. As a consequence of this, the AC field lends itself better to the constant demulsification process. The demulsification process in high electric fields (AC) was tested using a continuously electrostatic dehydrator under a variety of conditions. Since the electrostatic principle on energetic particles causes an increase in electrostatic force between droplets and since the droplets deform, the water separation efficiency (WS%) rises as the field strength is increased. The majority of the rise in WS% that may be attributed to temperature is likely due to a decrease in oil viscosity. Within the parameters of their experiment, the WS% increased as contact time increased. The authors reached less than 3% weight of latent water content in the demulsified emulsion under the experimental circumstances that were selected for this study.

Aryafard and colleagues (70) studied how the pressure drop in the mixing valve impacted the efficiency of dehydration and desalting. Simulation results show that elevating the pressure drop in the mixing valve accelerates the collision between emulsion drops and fresh water, leading to an adjustment in droplet size distribution towards smaller droplets and enhancing the stability of the emulsion. The results of their simulation indicated that an increase in the pressure drop of the mixing valve from 1.37 to 2.06 bar (20 to 30 psi) decreased the dehydration efficiency by 0.3%. In a related topic, Hosseinpour and his colleagues (77) found that increasing the standard mixing valve's pressure drop from 0.8 bar to 1.2 bar made the water cut at the outflow of the desalting process go up from 0.088% to 0.098%. Tahouni and colleagues (78) calrified that increased pressure drops in mixing valves result in smaller water droplets, impacting the desalter's efficiency in two contrasting ways.

Al-Otaibi and his coworkers (28) clarified that the water cut (W/C) efficiency of the dehydration stage rises as the gravity gap between oil and water widens. The asymptotic behavior of W/C efficiency is caused by the water droplets being too tiny to settle out. Over 40% of these droplets are too tiny to escape from the thin layers enclosing them. These thin films produce what is defined as a "tight emulsion." It is an emulsion with extremely tiny droplets of less than 10 microns that are difficult to separate.

Bessler and Chilingarian (27) showed that the gravity effect is so significant that a greater density difference between water and oil makes the separation simpler, while a smaller difference makes it more difficult. The size of water droplets has a big effect on how fast they separate and settle due to the fact that larger droplets fall faster (Stokes' law governs), which speeds up the process of coalescence into larger droplets (30).

2.3 Crude Oil Desalting

Biglari and colleagues (79) simulated the desalting unit of crude oil to achieve the specified water and salt levels in the outlet stream of oil. They concluded that there is a requirement for a second stage of desalting to achieve the desalting criteria for a particular PTB salt in the feedstock..

Rahmani and colleagues (80) found that based on the results of the sensitivity analysis conducted in Iran's oil field desalter model, the ideal temperature point for separation is 90 °C combined with 10% wash water. In contrast, the ideal point for separation in terms of wash water ratio was found at 100 °C and 8.3% wash water. Depending on the cost of energy and wash water, either of the two recommendations can be used to retrofit the desalter.

Fetter Pruneda and coworkers (81) developed mathematical models to replicate the variations in crude oil density, conductivity, and viscosity based on temperature, which are crucial elements in the desalting procedure. They showed that increasing the temperature of the process yields diverse results, whereas a decrease in crude oil density and viscosity allows for a higher processing rate as water droplets settle faster within the oil phase, providing an advantage. Additionally, the conductivity of crude oil increases exponentially with temperature, leading to a higher rate of power consumption (a disadvantage).

Tahouni and colleagues (78) found that as temperature rises, the density difference between water and oil, viscosity, and surface tension decrease. The

decrease in density difference has a negative impact due to the decreased speed of water droplets (sedimentation), reducing the water removal efficiency (Stokes law). While the reduction in viscosity and surface tension improves water removal, the lower viscosity of the oil phase increases sedimentation speed and collision velocities of water drops in desalter (Stokes' law states that the speed of drops is directly proportional to the density difference between oil and water and inversely proportional to the viscosity of the oil phase). The authors clarified, for their crude oil under study, that the viscosity and surface tension have a greater impact than the density difference on improving water removal efficiency. As a result, the desalter's water and salt removal efficiency improves as the temperature rises.

Thro and Arnold (82) worked with real field data for one set of circumstances, and reaching that potential response to other conditions of operation can be predicted. They provide a standard methodology for designing oil treatment plant facilities. A correlation is provided for use in the absence of any additional information. They are calculating the size of water droplets that need to be extracted from the oil to get the target of the basic sediment and water (BS&W) concentration. This correlation is based on both the data gathered in the field and the inferences drawn from design curves. According to this correlation, the horizontal operating area in the treater vessel increases with flow rate and crude oil viscosity while decreasing with specific gravity and square minimum water droplet diameter. This correlation makes it possible for designers to choose treater dimensions and a treatment temperature that will produce the required BS&W content because the droplet diameter is a factor of the required BS&W and viscosity. The researchers present an approach to selecting a treater size that accounts for variables such as the specific gravity of crude oil and water, the viscosity of the oil to be treated, and the temperatures at which the treatment will take place.

Vafajoo and colleagues (1) investigated the influence of specific operational parameters like demulsifier dosage and pH of the emulsion on the desalting effectiveness of crude oil. They concluded that an increase in demulsifier concentration necessitates a reduction in temperature; also, a rise in the pH of the emulsion has been shown to improve the desalting efficiency.

Khalaf and Rajab (83) clarified that raising the surfactant dose improved desalting efficiency and that a surfactant dosage of 10 ppm yielded the highest desalting efficiency. It has been observed that when the toluene-to-surfactant

mixing ratio is increased, the desalting effectiveness decreases because more asphaltene molecules are adsorbing onto the surface of water droplets. By creating viscoelastic interfacial films, emulsion stability is improved.

Akbarian and colleagues (84) studied how changing the current frequency affected the electric field strength, the voltage applied to the emulsion, the size distribution of water droplets, and the water cut in the recovered oil. The simulation findings show that the electric field strength is improved by raising the current frequency. The amount of water in processed crude oil is reduced as well. The findings demonstrated that the electrodes and emulsion acted as a capacitor as well as a dielectric substance, respectively, and that an electric field was generated between the electrodes when the power was switched off. And it seemed that as the distance between the electrodes grew, the off-time period grew as well, along with the applied voltage and the intensity of the electric field between the electrodes. It seemed that raising the temperature made the emulsion more conductive and weakened the electric field between the electrodes, but it also reduced the viscosity of the emulsion and boosted the dehydration process.

Separators utilize the electric field strategy to improve the process of separation of emulsion, working on the assumption that raising the electrical field strength reduces the retention time of coalescence. Modifying the standard coalescence equipment to include two adjacent metallic electrodes separated by a variable distance in order for the effects of di-electrophoresis to be insignificant, the droplet size-to-electrode length ratio must be as small as possible, for an electric field that is perpendicular to the interface, a high-voltage power source can be used. When DC electric field is applied, the residence time can decrease as the value of the electric field increases. When AC electric field is applied, the retention time is influenced by both the amplitude and frequency of the AC input (85–89).

Kavehpour (90) noticed by numerical modeling that the creation of a Taylor cone (the conical shape of the liquid emerging from a capillary under high voltage) is driven by the electric field at the gap, which reaches very high values as the space between the drop and the interface decreases. A Taylor cone is formed because of the strong electric field created by the oscillating field at the gap. An immediate rupture in the film will result from the cone's impact. Another important aspect that occurs in electrocoalescence is that the electric field forms secondary drops. The

supplied electric field causes an upward shear force at the interface between the coalescing droplets and the surrounding dielectric liquid.

Ibrahim and Sami (91) carried out their study with two different kinds of Iraqi crude oil used in the tests: Basra crude oil and Naft Khana crude oil. 7 vol % ethanolamine was added to the wash water to increase the droplets coalescence in order to improve dehydration and desalting process. Nonetheless, the separation of Basra crude oil from the wash water remained challenging. With heavy crude (Basra crude), the desalter water droplet settling the rate needed to be increased, and the crude oil salts needed to be diluted by using a higher wash water rate (more than 20 vol%). The researchers clarified that natural emulsifiers found in heavier oils (Basra crude) are more effective in preventing water droplet coalescence and encouraging the creation of stable emulsions in the desalter than those found in lighter crudes (Naft Khana crude).

3. MATERIALS AND METHODS

This chapter describes and explains the materials, methodology applied, and approach followed in the thesis on the desalting crude oil process:

1. Data gathering.
2. Laboratory experimental test.
3. Simulation of the Process.

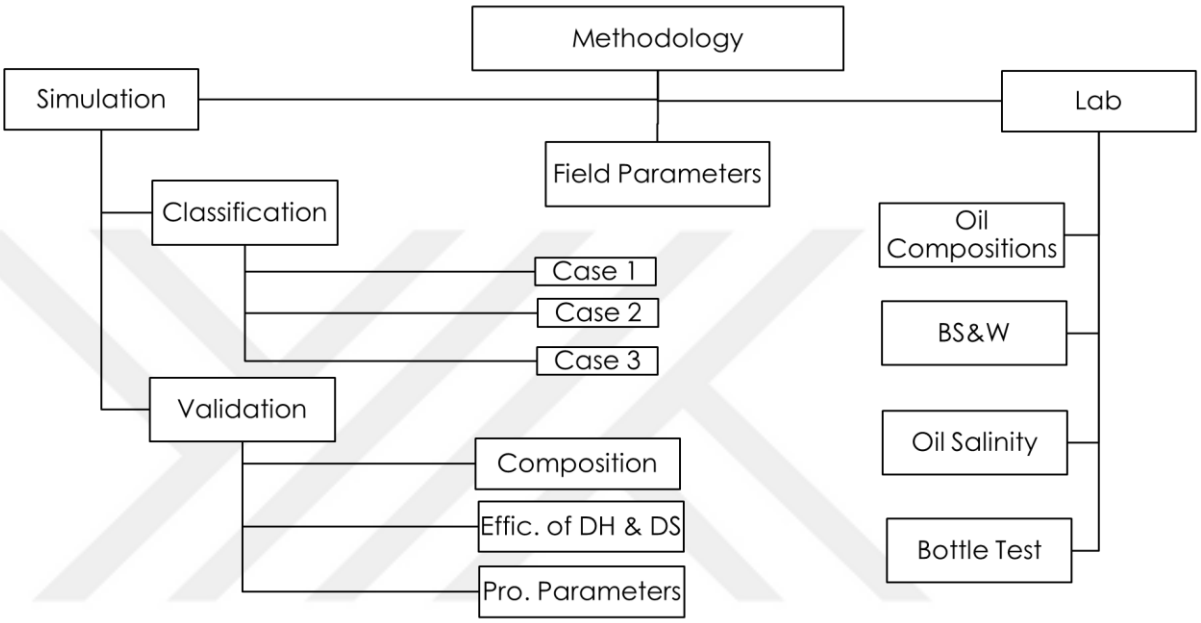

Figure 3.1 Hierarchy of desalting improvement methodology.

3.1 Data Gathering

The samples used for the creation of data to build a flowsheet simulation model of a crude oil desalting and dehydration process were collected from the oil and effluent water coming from one of the Basra fields in the south of Iraq, specifically from a crude oil treatment train inside the degassing station of a representative field. Crude oil samples were gathered from the oil sampler points of the separator train from the following locations of the plant shown in **Figure 3.6**:

1. Inlet manifold (flowline 1).
2. 1st stage oil outlet (flowline 2).
3. 2nd stage oil outlet (flowline 5).
4. Dehydrator oil outlet (flowline 7).
5. Desalter oil outlet (flowline 8).

Effluent water samples gathered from sampler points of train as follow:

1. 1st stage water outlet (flowline 12).
2. 2nd stage water outlet (flowline 13).
3. Dehydrator water outlet (flowline 14).
4. Desalter water outlet (flowline 15).

3.1.1 Investigated Variables

To investigate the impact of operational parameters, it is necessary to maintain all other variables at constant values while changing the parameter under research. This will allow for a comparison and analysis of the main effective results, like the flow rate of desalted oil by unit of barrels per day (bbl/day), gas flow rate by unit of million standard cubic feet per hour (MMSCFH), outlet salt concentration by unit of pounds of salt per thousand barrels of crude oil (PTB), and volumetric water content (V%) of treated oil, to reach the optimum operating conditions. **Table 3.1** below shows the conditions of the crude oil under research.

Table 3.1 Crude oil conditions to the train.

Inlet Variable	Value	Unit
Crude Oil Flow Rate	116834	bbl/day
Temperature	50	°C
Pressure	41.5	barg
Wash Water	3154 ≈ 21	bbl/day m^3/h

The key variables that significantly impact the efficiency of desalting are: the volume of desalted oil (bbl/day), the temperature of crude oil at each stage of the crude oil train (°C), the salt concentration at each stage of the crude oil train (PTB), the amount of chemical demulsifier used (ppm), and the proportion of fresh water added (%). The efficiency of crude oil treatment is contingent upon the specific design and operational parameters of the system, such as the configuration of the separators, the interface levels of oil and water, and the capacity of the pumps. Consequently, factors like the residence time of oil within the vessel and temperature are inherently limited by the design itself. Still, the main focus of the study of this thesis is on the amount of salt in the crude oil that comes out of all the stages of the train, such as the first stage, second stage, dehydrator, and desalter.

Furthermore, the composition analysis of crude oil is used to define the feed for the model of the software for flow sheet simulation.

3.2 Laboratory Analysis of the Field Collected-Samples

The main material and compositional analyses implemented were:

1. Crude oil composition.
2. Basic sediment and water of crude oil.
3. Salinity of crude oil.
4. Demulsifier dosage.

All the lab analysis work was done in the main laboratory of the Basra Oil Company (BOC).

3.2.1 Crude Oil Compositions Analysis

Gas chromatography (GC) was used as a fast and versatile method for simulated distillation (SimDist). High-temperature gas chromatography (HTGC) using SimDist methods may analyze substances with boiling points ranging from 35 to 750 °C. This range corresponds to the boiling points of n-alkanes, specifically from C_5 to C_{120} (92). An Agilent 7890A Gas Chromatograph (**Figure 3.2**), was utilized to analyze crude oil samples (distillate) in order to determine the fractional compositions following the ASTM D2887, IP 321 standard method, which is designed for assessing the boiling range distribution of petroleum fractions. A capillary gas chromatographic column (CP-SimDist UltiMetal) from also Agilent Technologies was used to separate the sample's hydrocarbon components according to their boiling points (up to C_{120}).

Figure 3.2 Agilent gas chromatograph (7890A).

3.2.2 Basic Sediment and Water (ASTM D4007)

The basic sediment and water (BS&W) content of crude oil samples were measured by centrifugation using a K60092 Koehler Instrument centrifuge (**Figure 3.3**) and following the ASTM procedure D4007, IP 359, which gives the volume of the water and sediment in the oil samples.

Figure 3.3 Oil test centrifuge (K60092).

3.2.3 Salinity of Crude Oil (ASTM D3230)

The salinity of crude oil samples was measured with the Salt-In-Crude by STANHOPE-SETA 99700-6 Analyser (**Figure 3.4**) according to ASTM procedure D3230, IP 265.

Figure 3.4 Salt-in-crude analyser (STANHOPE-SETA).

3.2.4 Demulsifier Bottle Test (ASTM D1796)

The bottle test method is employed to determine the optimal dosage of a chemical demulsifier in a production plant (i.e., the minimum ppm required to break down the emulsion). This is achieved by evaluating the efficiency of water separation in crude oil emulsions.

3.2.4.1 Equipment

1. 1000 ml glass tubes.
2. Water bath.
3. Tube rack.
4. Pipette.
5. Stopwatch.

3.2.4.2 Materials

1. Crude oil samples
2. Chemical demulsifier EPT-# (PID-#) by Schlumberger .

3.2.4.3 Testing Procedure

Samples of crude oil emulsions were collected from the production header of the production plant prior to the introduction of any chemicals. It's important to mention that the tests were done on the same plant, so the aging scenario for crude oil was not considered. The container was rotated for a duration of 30 seconds in order to re-homogenize the crude oil emulsion. Then, the crude oil emulsion was poured into glass tubes with a capacity of 1000 ml, ensuring that the tubes were filled to their maximum capacity at room temperature. Various concentrations of demulsifier (0, 10, 13, 16, 19, 25, and 30 ppm) were added to the emulsion tubes by the pipette. The manual mixing of the chemical demulsifier and emulsion was conducted by shaking the tube for 30 seconds. Each tube was carefully positioned vertically in a tube rack and thereafter immersed in a water bath for nearly 10 minutes until it reached 80 °C, as shown in **Figure 3.5**. After the samples reached the required temperature, they were removed out of the water bath. After 20 minutes, the percentage of separated water in each tube was measured.

Figure 3.5 Water bath.

3.3 Simulation of the Dehydration/Desalting Process

Aspen HYSYS software (version 10) is used to create process simulations of an existing crude oil desalting and dehydration train. The simulations are based on real data about the physico-chemical properties of the crude samples that were collected from plant, as well as information about the equipment design, operation conditions, and other factors. The process flow diagram for simulations is classified into three cases:

- Case 1 is given in **Appendix 1: Process Flow Diagram for Simulation Case 1**, which represents the flow sheet based on which the results have been calculated by Aspen HYSYS (the normal operation conditions).
- Case 2 is given in **Appendix 2: Process Flow Diagram for Simulation Case 2**, which represents the flow sheet based on which the results have been calculated by Aspen HYSYS (improvement of the temperature and pressure).
- Case 3 is given in **Appendix 3: Process Flow Diagram for Simulation Case 3**, which represents the flow sheet based on which the results have been calculated by Aspen HYSYS (improvement of the fresh water flow rate).

It's important to mention that all these above-mentioned simulation cases were built independently of equipment size. The main operation conditions of the 3 cases shown in **Table 3.2** below.

Table 3.2 Operation conditions of simulation cases.

Property	Case 1	Case 2	Case 3
Crude oil feed rate (bbl/day)	116834	116834	116834
Mass flow (kg/h)	706694	706694	706694
Crude oil salt content (PTB)	18192	18192	18192
Crude oil temperature (°C)	50	80	80
Crude oil pressure (barg)	41.5	14	14
Fresh water flow rate (m^3/h)	21	21	16

3.3.1 Feedstock Stream

To initiate the modeling of the crude oil train process, the initial stage entails establishing the composition of the feed supplied to the train. In order to achieve this objective, HYSYS incorporates a highly extensive integrated databank that allows for the selection of chemical components to construct the feed components. It's critically important to add the light hydrocarbon parts from the HYSYS databank source, such as C_1 to C_6, water (H_2O), nitrogen (N_2), carbon dioxide (CO_2), and sodium chloride (NaCl), to the simulation of crude oil feeds. However, it is commonly seen that for heavier crude oil compositions, the feedstock must be handled using the pseudo-components that are not readily accessible in the existing databank. The comprehensive examination of data is commonly known as the Crude Assay. The accuracy of the crude assay preparation directly impacts the fidelity of the crude simulation and consequently enhances the reliability of the simulation findings. **Table 3.3** shows the molar fraction of the compositions of the field data (inlet manifold sample), which was then used as the simulation feed stream. In addition, the properties and operation conditions of the field plant as shown in **Table 3.4** are attached to the simulation feed stream for a more accurate and accepted result. Finally, it is important to mention that the crude oil sample analysis demonstrated a non-sour attribute, so this is why there are no sulfide components in the simulation of the feed.

Table 3.3 Compositions of the feed stream and its component mole fractions.

Composition	Mole Fraction	Molecular Weight (g/mol)
H_2O	0.82191	18
N_2	0.00071	28
CO_2	0.00129	44
Methane	0.05893	16
Ethane	0.01441	30
Propane	0.01005	44
i-Butane	0.00722	58.1
n-Butane	0.00243	58.1
i-Pentane	0.00351	72.1
n-Pentane	0.00273	72.1
n-Hexane	0.00452	86.1
C7*	0.00280	96
C8*	0.00255	109
C9*	0.00238	123
C10-15*	0.01095	173.6
C16-20*	0.00621	261.4
C21-27*	0.00590	341.9
C28-35*	0.00416	442.3
C36-47*	0.00347	546.4
C48-80*	0.00266	769.3
NaCl	0.03121	58.4

Table 3.4 Feed properties and operation conditions of the plant.

Property	Value	Property	Value
Crude oil feed rate (bbl/day)	116834	Density @ Std. Cond (kg/m^3)	913.1
Crude oil temperature (°C)	50	API	33.2
Crude oil pressure (barg)	41.5	Molar Flow (kgmol/h)	22021
Vapor / Phase Fraction	0.0655	Mass Flow (kg/h)	706694
GOR (SCF/bbl)	895	Molecular Weight	32
Crude oil water cut (%V)	39	Fresh water (% of crude feed)	3
Crude oil salt content (PTB)	18192	Fresh water temperature (°C)	25

3.3.2 Fluid Package Property

The HYSYS software program employs thermodynamic principles and utilizes a fluid package (equation of state) to accurately compute the parameters of the intended process. The Peng-Robinson (PR) property method is widely regarded as the most recommended fluid package for studying processes related to nonpolar or mildly polar mixtures like hydrocarbons and light gases (93). Peng-Robinson equation of state, thus, was used in this this study due to its capacity and

characteristics to handle hypothetical (pseudo) components of crude oil, also its ability to operate over a wide range of pressure and temperature conditions (94,95).

According to simulation basis guide of aspen technology the formulations used in HYSYS for the PR equations of state as follows:

$$P = \frac{RT}{V-b} - \frac{a}{V(V+b)+b(V-b)} \tag{11}$$

Where the variables are defined as follows:

P: pressure of the system,

T: temperature,

V: molar volume,

R: gas constant,

a, b: substance-specific constants.

The substance-specific parameters a and b are calculated using the critical properties of the composition, like temperature (T_c), pressure (P_c), molar volume (V_c), and acentricity (ω) (96). See **Appendix 6: Critical properties of crude oil compositions**, which contains all the critical properties of crude oil compositions used in the simulation of this study.

3.3.3 Salt Concentration

The measurement of salt concentration in crude oil feed is often expressed as a pound of sodium chloride (NaCl) per 1000 barrels of crude oil, commonly referred to as pounds per thousand barrels (PTB). Based on the crude oil samples from inlet manifold that were analyzed in the lab, it was found that the concentration of salt in the inlet feed was 18192 PTB. The equation below is the spine of salt concentration calculation. As an example, the salt concentration of inlet feed 18192 PTB, and the liquid volume flow rate of inlet 116834 bbl/day used in this equation to find the salt mass flow in the inlet 40170 kg/h. This real field data was used as the property of the feed stream in the simulations. The value of PTB was integrated to the simulation package using spreadsheet calculations.

$$Salt\ (PTB) = \frac{Salt\ mass\ flow\ \left(\frac{kg}{h}\right) \times 2{,}2046221 \left(\frac{Ib}{kg}\right) \times 24\ \left(\frac{h}{day}\right)}{Liq,vol\ flow\ \left(\frac{bbl}{day}\right)} \times 1000 \tag{12}$$

3.3.4 Process Description of the Crude Oil Train

Understanding the dehydration and desalting processes necessitates a comprehensive description of the crude oil train **Figure 3.6**, spanning from the manifold to the storage system. Sub-sections below provide a depiction of the process for each component of the crude oil train.

3.3.4.1 First Separation Stage

Crude oil flows from the manifolds to the 1st stage separator through a control valve under flow rate control (flowline 1). The separator function a preliminary three-phase separation: crude oil, gas, and water. The 1st stage separator is a horizontal vessel equipped with adequate internal devices, providing high separation efficiency. It's designed to work at different pressure levels to match the phasing of new train facilities. The gas from the 1st stage separator is sent to the high pressure (HP) flare network (flowline 10), while separated water is sent, under interface level control, to the produced water treatment system (flowline 12).

3.3.4.2 Oil Pre-heating and Oil Heating

The outlet oil of the 1st stage separator is routed under level control to the oil pre-heater (flowline 2) and then to the oil heater (flowline 3) in order to facilitate further separation in the 2nd stage separator and guarantee a temperature of 95 °C at the dehydrator. The oil pre-heater system consists of two identical shell and tube heat exchangers (one working and one stand by) arranged in series. The outlet oil from the 1st stage separator (flowline 2) enters the tube side of the pre-heater to recover the heat from the treated oil (shell side) coming from the outlet desalter (flowline 8). The oil heaters also consist of two identical shell and tube heat exchangers arranged in parallel (one working and one stand by). In case of complete bypass of the oil pre-heater for maintenance or malfunction, the two oil heaters are arranged to work in parallel mode to cover the required total duty.

3.3.4.3 Second Separation Stage

The oil that has already been heated flows through the oil heaters, where it is heated even more by a hot oil stream. It then flows into the 2nd stage separator (flowline 4), which, like the 1st stage, is a horizontal vessel with appropriate internal devices to ensure high-efficiency separation. The gas from the 2nd stage separator is sent to the low pressure (LP) flare network (flowline 11). A differential pressure control is provided between the separated gas outlet line of the 2nd stage and the

separated oil outlet line from the desalter in order to prevent vapor separation in the desalter.

3.3.4.4 Dehydration Stage

The desalting feeding pumps (one working and one stand by) transport separated oil from the 2nd stage (flowline 5) to the dehydrator while maintaining level control (flowline 6). The separated water leaves the 2nd stage under interface level control and flows to the produced water treatment system (flowline 13). The heated oil coming from the 2nd stage by means of the desalting feed pumps is first mixed with the produced water recycled from desalter vessel (flowline 15), then it enters, from the bottom, the electrostatic dehydrator, where oil/water separation takes place. Injection of demulsifier agent upstream of the mixing valve is foreseen in order to break the emulsions and facilitate the oil/water separation inside the dehydrator (sometimes the demulsifier is injected in the manifold to give more resistance time to break the emulsions and increase the oil/water separation). The electrostatic dehydrator is a horizontal vessel equipped with high-voltage electrodes in order to aid the separation between produced water and crude oil. The separated water, leaving the bottom of the dehydrator (flowline 14), is routed, under level control, to the produced water treatment, passing through the effluent water/wash water economizer (one working and one spare) in order to heat up the wash water coming from the wash water system (flowline 16).

3.3.4.5 Desalting Stage

Separated oil, leaving from the top of the dehydrator (flowline 7), is mixed with the wash water coming from the effluent water/wash water economizer (flowline 16) just upstream of the mixing valve and enters the electrostatic desalter from the bottom, where oil/water separation takes place. The electrostatic desalter is a horizontal vessel equipped with high-voltage electrodes. Separated water from the bottom of the desalter (flowline 15) is recycled back to the dehydrator, under interface level control, by means of two recycle water pumps (one working and one stand by). In the case of a high interface level in the desalter, excess water is delivered to the produced water treatment through a dedicated control valve operated by the desalter interface control level. In normal conditions (i.e., salt content and water cut in the accepted range), the treated (desalted) crude oil from the desalter is sent to the oil pre-heater (flowline 8) to heat up the oil inlet of the

2nd stage prior to entering the next step of the process (flowline 9), which is storing and exporting.

The dehydrator and the desalter are equipped with dedicated bypasses in order to allow maintenance of the equipment without taking out of service the whole oil separation train; in this case, the treated oil can be diverted to the off-spec oil System if the oil content specification is not met.

When using chemical demulsifiers, it is common to find an injection point before each stage of the process. This gives the process the flexibility to add the demulsifier where it needs to destabilize the emulsion, which depends on the properties of both the oil and the demulsifier.

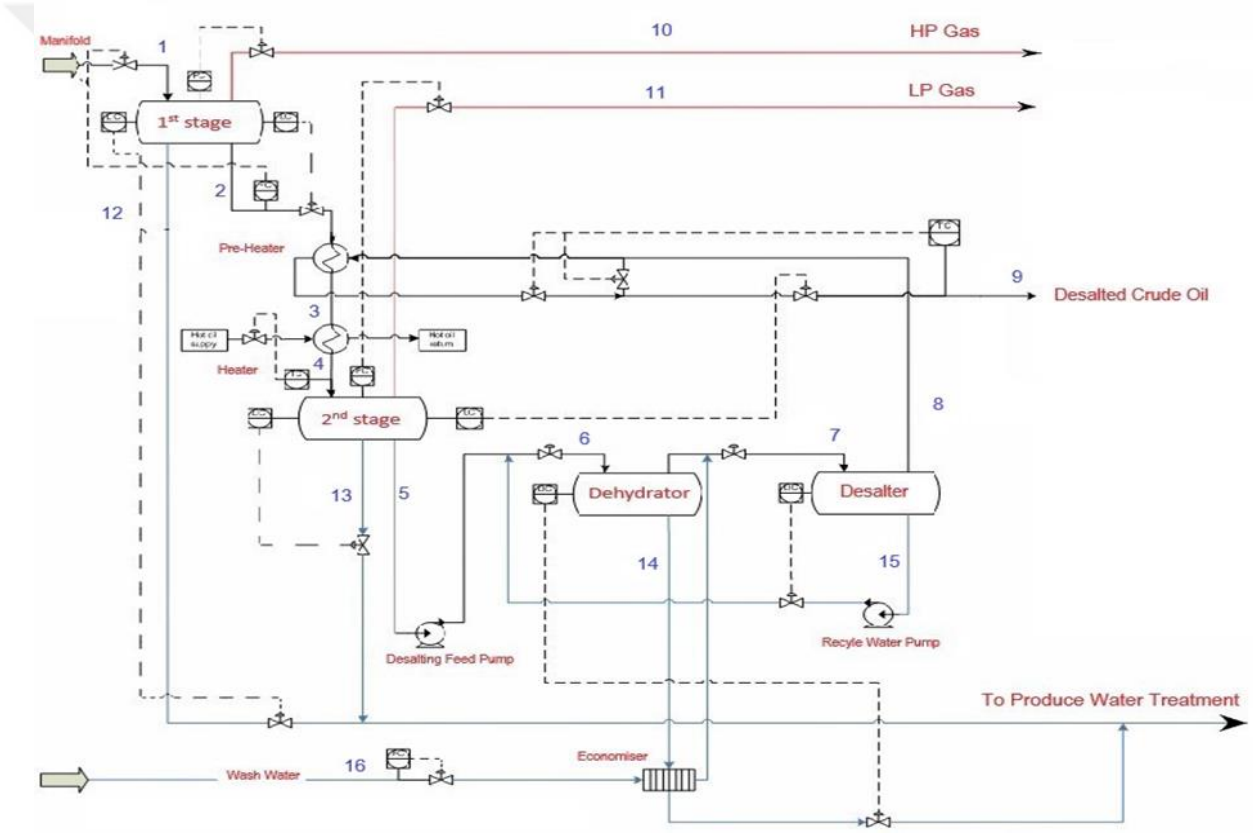

Figure 3.6 Process flow diagram of a typical crude oil Dewatering/Demulsification train.

3.3.5 Simulation Input Data for the main equipment

This section gives a short explanation of the input data and functions of the main pieces of equipment used in the crude oil train simulation process by Aspen HYSYS software, which is based on real plant data. The goal is to make the simulation easier to understand. The simulation encompasses a series of pieces of equipment arranged in accordance with the process flow design, with consideration

given to the sequential order of fluid flow. All the equipment details below are shown in the **Appendix 1: Process Flow Diagram for Simulation Case 1**, which represents the flow sheet based on which the results have been calculated by Aspen HYSYS.

3.3.5.1 1st Stage Separator (VS-001)

Based on the real field separation and treatment plant data under the scope of this study, the 1st stage is modeled as a three-phase separator, with operating parameters set at a temperature of 50 °C and a pressure of 36.5 barg. The structure in question is characterized by its flat, horizontal cylindrical shape, with input dimensions of 3.6 m in diameter, 17.5 m in length, and a volume of 178.1 m^3. The input feed of the 1st stage separator is 116834 bbl/day of crude oil feed from the inlet manifold through stream-line 1, which has a temperature of 50 °C and a pressure of 41.5 barg. The flow control valve FV-001, set with a pressure drop of 5 barg, regulates this flow.

3.3.5.2 2nd Stage Separator (VS-002)

The second stage, like the first, is simulated as a three-phase separator, operating under settings of 95.6 °C and 4.8 barg for temperature and pressure, respectively. The object in question is characterized by a flat, horizontal cylindrical shape with dimensions of 3.1 m in diameter, 15 m in length, and a volume of 113.2 m^3. The separator received the heated oil from the heater through stream-line 4, controlled by a temperature control valve (TV-001).

3.3.5.3 Oil Desalting Feed Pump (PA-001)

The oil outlet from the 2nd stage separator, namely stream-line 5, is transferred to the dehydrator using the oil desalting feeding pump PA-001. This pump operates with a suction pressure of 4.8 barg and discharges at a pressure of 11.35 barg. The liquid volume flow rate of the pump is 365 m^3/h.

3.3.5.4 Dehydrator (VU-001)

The electrostatic dehydrator is represented in the simulation as a three-phase separator, but its physical configuration is two-phase. The temperature and pressure operating conditions are set at 95 °C and 9.8 barg, respectively. The vessel in inquiry exhibits a planar, horizontal, cylindrical shape, measuring 3 meters in diameter and 11.8 meters in length, and possessing a volumetric capacity of 83.4 cubic meters. Recycled water from the desalter vessel stream-line 15C is mixed with the oil outlet from the desalting feed pump stream-line 5A.

3.3.5.5 Effluent Water/ Wash Water Economizer (HB-001)

The utilization of a shell and tube heat exchanger economizer facilitated the elevation of the wash water temperature from an initial value of 25 °C. Stream-line 16 of the system supplied the wash water, which was regulated by the flow control valve FV-006. The aforementioned target is accomplished by employing the heated, generated water acquired from stream-line 14 of the dehydrator.

3.3.5.6 Desalter (VU-002)

The electrostatic desalter, like the dehydertor, is simulated as a three-phase separator in the simulation, despite its physical configuration being a two-phase system. The prescribed operating conditions for temperature and pressure were set at 93 °C and 8.7 barg, respectively. The indicated vessel is characterized by a flat, horizontal, cylindrical shape. Its dimensions include a diameter of 3 m, a length of 11.8 m, and a volumetric capacity of 83.4 m^3. The outlet oil from the dehydrator stream-line 7 is mixed with wash water from the economizer stream-line 16B. Wash water is set at 74 °C, 9.8 barg, and a flow rate of 21 m^3/h (i.e., the wash water rate is 3% of the total volume of feed) to be sent to the desalter through the mixing valve PDV-002. The pressure differential valve is adjusted to achieve a differential pressure of 1 barg, facilitating an increased level of mixing inside the system. The desalter does not exhibit gas separation, namely in the simulation as pseudo-vapor.

3.3.5.7 Recycle Water Pump (PA-002)

The effluent water discharged from the desalter, referred to as stream-line 15, is conveyed to the dehydrator through the utilization of the recycle water pump PA-002. The pump simulated in question functions by utilizing a suction pressure of 7 barg and afterwards discharging at a pressure of 12.35 barg with a volume flow rate of 23.7 m^3/h.

4. RESULTS AND DISCUSSION

4.1 Simulation Validation

In order to validate the simulation performed in this work, a comparison was made between the samples and the HYSYS simulation. This comparison was done for three aspects: composition, efficiency of the dehydrator and desalter, and process parameters.

4.1.1 Compositional Similarity

In order to ensure the validation of the simulation conducted in this thesis, the desalted oil (oulet oil from desalter) compositions of the plant field were compared with their counterparts simulated by Aspen HYSYS (i.e., the compositions of the outlet oil from desalter in case 1), as shown in **Figure 4.1**. Based on the mole fraction data presented in this comparison **Table 4.1**, it can be observed that the similarity results obtained using HYSYS exhibit an acceptable degree of agreement (matching) with the field data (i.e., more than 97% of comparison similarity for all compositions except one).

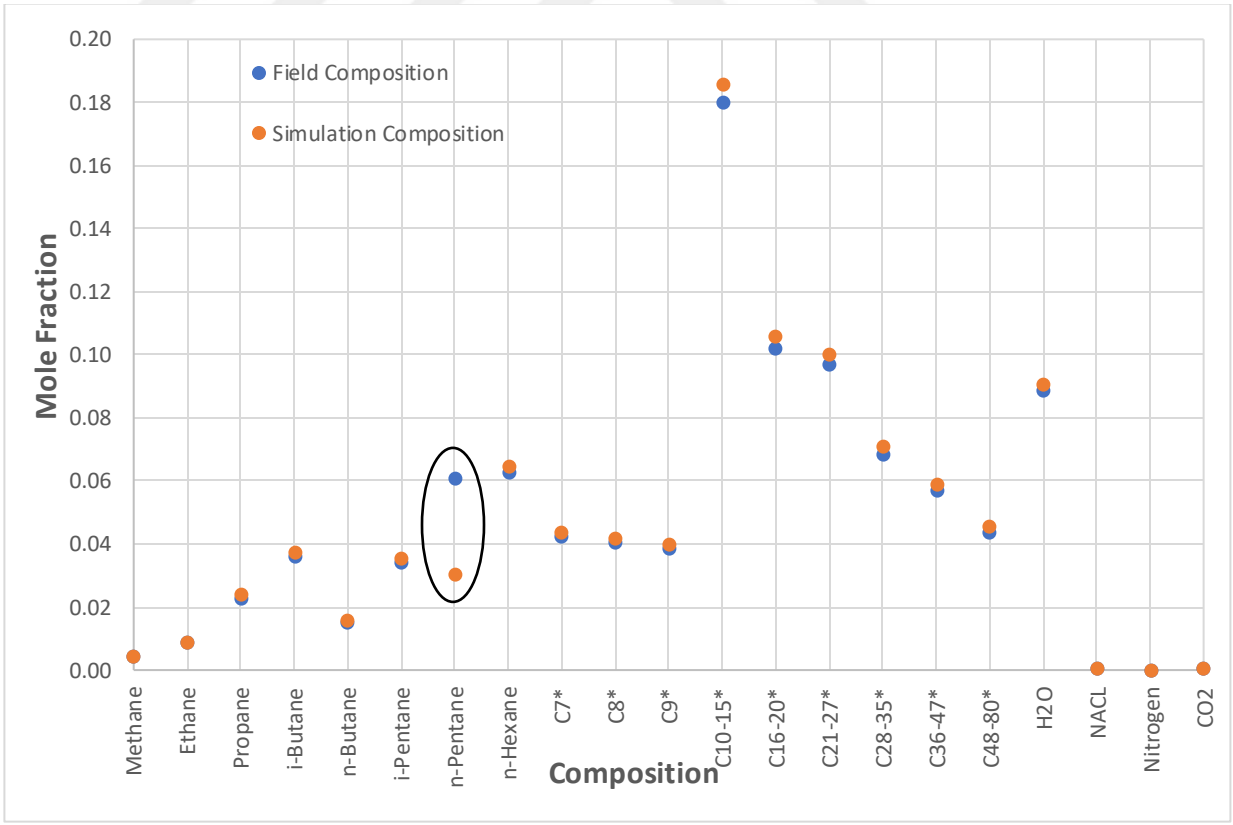

Figure 4.1 Compositional similarity of the desalted oil (Desalter outlet) between the HYSYS simulation and real field data.

The graphic illustrates a significant disparity between the simulation result (0.03002) and the laboratory field data (0.06045) for n-Pentane only. According to the deep compositional investigation, it's clear that the n-Pentane segment is difficult to measure because of its co-eluting with varied compositions. Along these lines, the sums were clustered together as lumped components. The relative proportions of oil compositions, ranging from C_7* to C_{80}*, exhibit a high degree of similarity between the field data and the simulation. Furthermore, tiny quantities of water (H_2O), sodium chloride (NaCl), nitrogen (N_2), and carbon dioxide (CO_2) are also present in **Table 4.1**. The fact that there were no big differences between the simulation and reality shows that the HYSYS simulation results are highly reliable and thus can be used as a reliable tool for making predictions in operations.

Table 4.1 Composition of the desalted oil for both HYSYS simulation and real field data.

Composition	Lab Data (Mole Fraction)	Simulation Data (Mole Fraction)	Similarity *
Methane	0.00391	0.00403	97 %
Ethane	0.00847	0.00876	97 %
Propane	0.02267	0.02374	95 %
i-Butane	0.03586	0.03705	97 %
n-Butane	0.01488	0.01538	97 %
i-Pentane	0.03407	0.03519	97 %
n-Pentane	0.06045	0.03002	201 %
n-Hexane	0.06240	0.06446	97 %
C7*	0.04202	0.04342	97 %
C8*	0.04027	0.04161	97 %
C9*	0.03845	0.03972	97 %
C10-15*	0.17977	0.18569	97 %
C16-20*	0.10201	0.10537	97 %
C21-27*	0.09683	0.10002	97 %
C28-35*	0.06837	0.07063	97 %
C36-47*	0.05699	0.05887	97 %
C48-80*	0.04364	0.04508	97 %
H_2O	0.08847	0.09050	98 %
NaCl	0.00008	0.00006	133 %
N_2	0.00001	0.00001	100 %
CO_2	0.00038	0.00039	97 %

$$* \text{Similarity } \% = \frac{\text{Lab Data}}{\text{Simulation Data}} \times 100$$

4.1.2 Efficiency of Dehydrator and Desalter

The simulation efficiency of the desalting and dehydration processes is compared with the actual efficiency of the crude oil train in the field to verify that the simulation model being used is accurate. The metric used to quantify desalting efficiency is denoted as pounds of salt (NaCl) treated per thousand barrels of crude oil (PTB). Comparing the simulation results and field measurement under steady-state conditions reveals a very close match between the simulated dehydration efficiency of 86.6% and the plant unit value of 86.9%. Regarding the desalting efficiency, the simulation demonstrates a positive deviation from field data, with values of 93.7% and 92.1%, respectively. The predicted salt concentration of HYSYS and the actual field data salt are 4.869 PTB and 4.907 PTB, respectively.

4.1.3 Process Parameters

To ascertain the validity of the model employed in this thesis, the projected simulation variables like flow rate (bbl/day), water content (%), and salinity (PTB) of the dehydrator and the desalter are compared with the actual field data. This comparison of variables, as shown in **Table 4.2** presents a highly accurate analysis of the error percentage, which confirms that the model accurately predicted the dehydration and desalting operations of crude oil.

Table 4.2 Comparison between HYSYS results and real field plant data.

Parameter	Field Data	Simulation Results	Difference % *
Crude Oil Feed (Stream 1)			
Flow rate (bbl/day)	116834	116834	0
Water content (% Vol.)	39	39	0
Salinity (PTB)	18192	18192	0
Dehydrator (VU-001)			
Inlet flow rate (bbl/day)	53214	53187	0.050
Inlet water content (% Vol.)	7.165	7.161	0.055
Inlet salinity (PTB)	440	445.7	-1.295
Outlet flow rate (bbl/day)	51214	51183	0.060
Outlet water content (% Vol.)	1.036	1.034	0.193
Outlet salinity (PTB)	60.72	60.39	0.543
Desalter (VU-002)			
Inlet flow rate (bbl/day)	52994	52969	0.047
Inlet water content (% Vol.)	6.859	6.854	0.072
Inlet salinity (PTB)	57.92	58.36	-0.759
Outlet flow rate (bbl/day)	50967	50994	-0.053
Outlet water content (% Vol.)	0.626	0.625	0.159
Outlet salinity (PTB)	4.907	4.869	0.774
Recycle Water (Stream 15)			
Flow rate (bbl/day)	3370	3370	0

$$* \text{Difference } \% = \frac{(\text{Field Data} - \text{Simulation Result})}{\text{Field Data}} \times 100$$

4.2 Simulation Results

In this section, an overview is presented of the results of each stage of the crude oil train simulation conducted using the Aspen HYSYS. **Appendix 1: Process Flow Diagram for Simulation Case 1,** taken from the HYSYS simulation, display the results in the following manner:

4.2.1 1st Stage Separator (VS-001)

The liquid volume flow rate through the inlet stream-line for the simulation is specified to be 116834 bbl/day (the field value 116834 bbl/day). Within this separator, the vapor (gas) stream-line 10 carried a flow rate of 1.663 MMSCFH, the heavy liquid (effluent water) stream-line 12 carried a flow rate of 270.1 m^3/h, and the light liquid (treated oil) stream-line 2 is directed to the pre-heater for further processing. The simulation salt results for the outlet oil and effluent water are 8440 PTB and 40217 PTB, respectively.

4.2.2 Oil Pre-heater (HA-001) and Oil Heater (HA-002)

The outlet oil from the 1st stage separator is directed through a level control valve (LV-001). The oil is operating at a temperature of 47.6 °C, a pressure of 7.2 barg, and a flow rate of 62281 bbl/day. To achieve crude oil heat exchange perfectly, first the oil is heated using the oil pre-heater HA-001, which is a shell and tube heat exchanger. The tube side of the exchanger is utilized to raise the temperature of the oil to 72.2 °C for stream-line 3. Subsequently, the oil is further heated using the oil heater HA-002, another shell, and a tube heat exchanger. The tube side of this exchanger was employed to increase the temperature of the oil to 95.6 °C for stream-line 4. This heating process was necessary to facilitate additional separation in the 2nd stage separator and ensure that the oil entering the dehydrator maintained a temperature of 95 °C. This temperature is crucial for achieving the desired fluid viscosity required for effective desalting. After being desalted in the desalter (stream-line 8), the oil goes through the shell side of the oil pre-heater HA-001 to lower its temperature and reach the right Reid Vapor Pressure (RVP) level. Moreover, a distinct type of thermally conductive oil, characterized by a

temperature range spanning from 200 to 260 °C, was circulated within the shell side of the oil heater exchanger.

4.2.3 2nd Stage Separator (VS-002)

The inlet oil flow rate through stream-line 4 is simulated to be 62281 bbl/day, where the gas separation occurs through stream-line 11 at a flow rate of 0.085 MMSCFH and the effluent water is produced through stream-line 13 at a rate of 88.1 m^3/h. The outlet oil is directed to the desalting feed pump PA-001. The simulation salt result of the outlet oil is 406.5 PTB, whereas the effluent water recorded 40383 PTB.

4.2.4 Dehydrator (VU-001)

Crude oil discharge from the desalting feed pump stream-line 5A, which operates at a temperature of 95.8 °C and a pressure of 11.35 barg, is combined with recycled water from the desalter vessel stream-line 15C. The recycled water is maintained at a temperature of 93 °C and a pressure of 11.35 barg. As shown in stream-line 6, which operates at a temperature of 95.4 °C and a pressure of 11.35 barg, the mixing valve (PDV-001) directs the oil and the recycled water toward the dehydrator. This pressure differential valve (PDV-001) is set to provide a pressure drop of 1.55 barg, which serves the purpose of enhancing the degree (intensity) of mixing oil with fresh water within the system. Gas separation is not observed in the dehydrator vessel, namely in the simulation as pseudo-vapor. The simulated inlet oil has a liquid volume flow rate of 51314 bbl/day, while the recycled water has a flow rate of 3367 bbl/day. Meanwhile, the effluent water is observed to flow through stream-line 14 at a volumetric flow rate of 23.8 m^3/h. The dehydrated oil, stream-line 7, is directed towards the desalter vessel to complete the process treatment. The simulated salt content value of the oil discharged from the dehydrator is 60.2 PTB, while the effluent water exhibited a recorded salt content of 6090 PTB.

4.2.5 Desalter (VU-002)

The dehydrated oil obtained from the dehydrator stream-line 7, operating at a temperature of 95.5 °C and a pressure of 9.7 barg with a flow rate of 51183 bbl/day, is mixed with the heated wash water from the economizer stream-line 16B. The economizer stream-line 16B operates at a temperature of 74 °C and a pressure of 9.8 barg with a volumetric flow rate of 3154 bbl/day (21 m^3/h). The stream-line 7A exhibits a mixed flow characterized by a temperature of 92.8 °C and a pressure

of 9.7 barg. This flow is maintained at a volumetric flow rate of 52969 bbl/day and is sent to the desalter through the mixing valve PDV-002. In the interim, the effluent water is sent through stream-line 15 with a flow rate of 23.7 m^3/h and subsequently reintroduced into the dehydrator for recycling purposes. The oil exit, referred to as stream-line 8, is directed into the pre-heater. Subsequently, upon undergoing a temperature reduction, desalted oil, known as stream-line 9, reached a temperature of 52.6 °C and a pressure of 5.6 barg. The simulation results show that the flow rate of desalted oil is 50994 bbl/day, while its salt concentration is 4.86 PTB with a water content of 0.62% volume. The effluent water demonstrated a simulated salt level of 842 PTB.

4.3 The Impact of Operating Conditions

It's necessary to maintain all other variables at constant values while investigating the effect of changing the parameter. The objective was to examine the impact of varying operating conditions (temperature, pressure, wash water flow rates, etc.) on the flow rate of desalted oil, gas flow rate, salt concentration, and water content of treated oil.

4.3.1 Temperature Effect

The manifold of the crude oil train facility typically exhibits a real temperature of approximately 50 °C, originating from various wells dispersed in the field. In the simulation, temperature of the feed to the 1st stage separator (VS-001) is changed in 3 °C increments (step size) from 20 to 80 °C (inlet flow rate, pressure, and wash water flow rate kept constant) to determine how different feed temperatures affect. As shown in **Figure 4.2** and the data presented in **Table 4.3** which was extracted from the HYSYS simulation, elevating the feed temperature (first stage temperature) results in a reduction in the desalted oil flow rate. This phenomenon can be attributed to the fact that certain hydrocarbons attain their saturation temperature under the prevailing operating pressure conditions, leading to their evaporation and transition into the gas phase. Consequently, it is anticipated that there is a decrease in oil production, accompanied by an increase in the quantity of gas generated. The case study of the simulation clarified that the change in temperature of the feed from 20 to 80 °C results in a slight increase in the gas flow rate from 1.714 to 1.877 (MMSCFH) and a corresponding decrease in treated oil flow rate from 51591 to 49680 bbl/day. The presence of crossing in the behavior of gas and oil curves can be observed in **Figure 4.2**. The observed phenomenon can

be attributed to the increase in energy acquired by hydrocarbon molecules with rising temperatures. As a result, a greater proportion of the lighter hydrocarbons undergo vaporization, leading to a decrease in the oil's flow rate. An elevation in the temperature of the feed has the potential to result in a marginal decrease in the true vapor pressure (TVP). Raising the temperature of the feed would result in a greater proportion of the light component readily vaporizing from the crude, thereby leading to a decrease in the TVP of the resultant product. In addition to the requirement of maintaining pressure for an extended duration, elevated temperatures contribute to the promotion of destabilizing effects resulting from Brownian motion. This phenomenon ultimately leads to a reduction in interfacial viscosity. Consequently, the separation process is facilitated due to disparities in density and polarity. Once again, this assumption is relevant in the context of achieving effective separation between oil-water emulsions.

It's important to mention that the coefficients of determination R^2 (the proportion of variation in the dependent variable that is predicted by the statistical model) of desalted oil flow rate and gas flow rate regarding the temperature variable are 0.962 and 0.910, respectively.

Table 4.3 Effect of various first stage temperatures on oil and gas flow rates.

Temperature (°C)	Desalted Oil Flow Rate (bbl/day)	Gas Flow Rate (MMSCFH)
20	51591	1.714
23	51571	1.714
26	51542	1.715
29	51504	1.716
32	51457	1.719
35	51401	1.722
38	51336	1.725
41	51262	1.730
44	51180	1.736
47	51090	1.742
50	50992	1.749
53	50886	1.757
56	50774	1.766
59	50655	1.776
62	50530	1.787
65	50399	1.799
68	50264	1.813
71	50124	1.827

Table 4.3 Continued.

74	49979	1.842
77	49831	1.859
80	49680	1.877

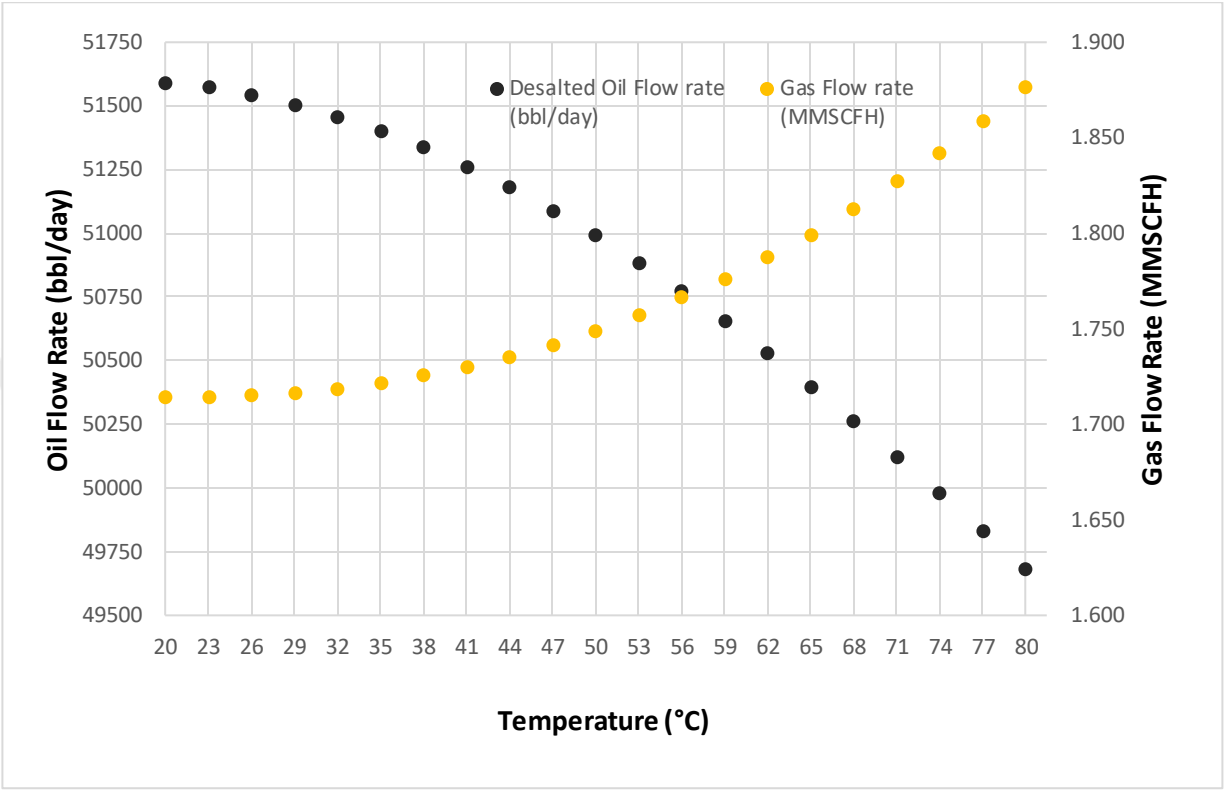

Figure 4.2 First stage temperature effect on oil and gas flow rates.

In a relevant context, the simulation has demonstrated a correlation between temperature variations (from 20 to 80 °C) and the concentration of salts in the produced oil. Namely, it's observed that the concentration of salt decreased from 4.979 to 4.641 PTB as the temperature changed. While the water content of the desalted oil remains constant regardless of temperature variations, as depicted in **Figure 4.3** and **Table 4.4**, this observation suggests that the temperature does not influence the water content fraction of the produced oil during the crude oil separation process. The separator effectively keeps resulting in a consistent water content fraction of 0.0062 at the outlet oil.

The explanation of that regarding the solubility of a specified solute depends on the temperature of the solution, indicating that the solubility of solutes, such as salt, exhibits an upward trend as the temperature rises (97,98). For a crystalline

solid, the electrostatic interactions between ions with opposite charges are frequently quite robust. It is noteworthy that NaCl (the main salt of crude oil) exhibits a remarkable ability to dissolve in water with a high increase in temperature (i.e., this can be attributed to the relatively high melting temperature of NaCl at 801 °C). This phenomenon is explained by the fact that the energy required to disrupt the bonds within an ionic crystal lattice is offset by the energy released when Na^+ and Cl^- ions form new connections with water molecules, resulting in enhanced stability. The high polarity of water molecules enables them to establish robust interactions with charge species. An additional element that can contribute to the facilitation of dissolution is the augmentation of entropy resulting from the liberation of ions from the lattice and their subsequent dispersion into the solution. The solubility of crude oil salt increases as temperature rises, due to the influence of entropy. Water's inability to form robust ion bonds clearly explains the limited solubility of NaCl in organic solvents. This can be understood by considering the salt hydration shells and the solute's capacity to establish a hydrogen bond with water (99).

It's important to mention that R^2 of salt concentration and water content regarding the temperature variable are 0.976 and 0.969, respectively.

Table 4.4 Effect of various first stage temperatures on salt and water content concentration.

Temperature (°C)	Salt Outlet (PTB)	Water Content Outlet (Fraction)
20	4.979	0.0063
23	4.973	0.0063
26	4.966	0.0063
29	4.957	0.0063
32	4.947	0.0063
35	4.936	0.0063
38	4.923	0.0063
41	4.909	0.0063
44	4.894	0.0063
47	4.877	0.0063
50	4.859	0.0063
53	4.841	0.0062
56	4.821	0.0062
59	4.801	0.0062
62	4.779	0.0062

Table 4.4 Continued.

65	4.757	0.0062
68	4.735	0.0062
71	4.712	0.0062
74	4.689	0.0062
77	4.665	0.0062
80	4.641	0.0062

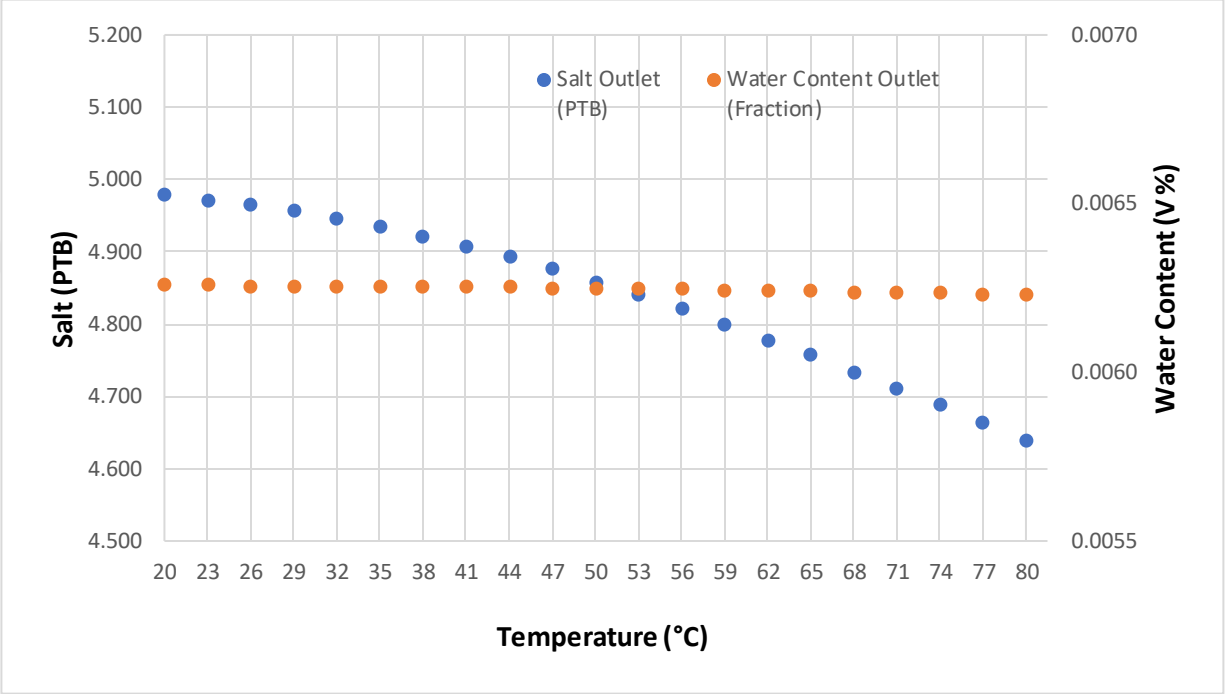

Figure 4.3 First stage temperature effect on salt concentration and water content.

4.3.2 Pressure Effect

The pressure observed in the manifold of the crude oil train facility is normally measured at 41.5 barg. In the simulation conducted, the feed pressure (first stage pressure) is varied in increments of 2 bar from 64 to 14 barg (inlet flow rate, temperature, and wash water flow rate kept constant). The objective is to examine the impact of different feed pressures on various parameters, namely the flow rate of desalted oil, gas flow rate, outlet oil salt concentration, and water content of treated oil. The findings are shown in **Figure 4.4** and in **Table 4.5**. Decreasing the feed stream pressure from 64 to 14 barg leads to an increase in the outlet gas flow rate from 1.205 to 1.752 MMSCFH, which is reflected in the reduction in oil volume from 52143 to 50948 bbl/day. **Figure 4.4** exhibits a notable occurrence of crossing in the behavior of gas and oil curves, as was the case in **4.3.1**.

Table 4.5 Effect of various first stage pressures on oil and gas flow rates.

Pressure (barg)	Desalted Oil Flow Rate (bbl/day)	Gas Flow Rate (MMSCFH)
64	52143	1.205
62	52176	1.219
60	52210	1.234
58	52244	1.248
56	52277	1.263
54	52310	1.278
52	52343	1.293
50	52375	1.309
48	52406	1.325
46	52437	1.341
44	52465	1.358
42	52492	1.375
40	52516	1.393
38	52537	1.411
36	52553	1.430
34	52564	1.449
32	52567	1.470
30	52560	1.491
28	52539	1.514
26	52500	1.538
24	52434	1.564
22	52332	1.592
20	52176	1.623
18	51960	1.659
16	51600	1.700
14	50948	1.752

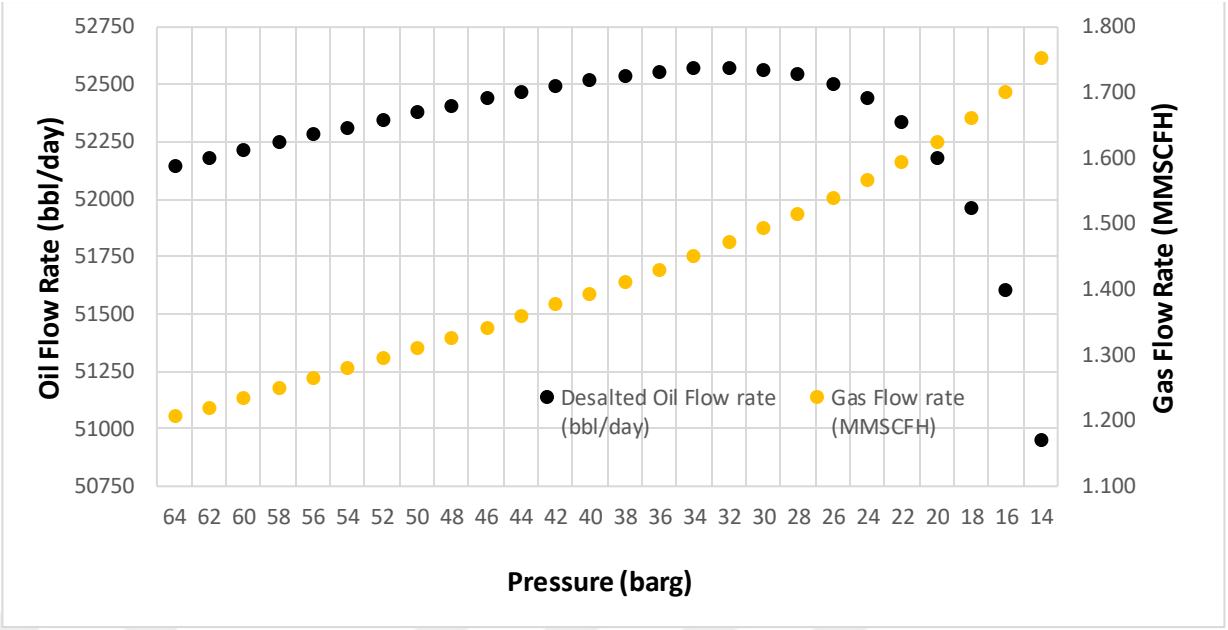

Figure 4.4 First stage pressure effect on oil and gas flow rates.

As can be seen from the results, there is a decrease in the salt content of the oil phase from 5.775 to 4.860 PTB in response to reduction in pressure. The water content of the desalted oil remains constant, irrespective of changes in pressure, as illustrated in **Figure 4.5** and **Table 4.6**. This finding implies that alterations in the pressure range investigated here do not have an impact on the proportion of water in the treated oil.

It is widely agreed that heavy oils are primarily created as light oil, which then undergoes decomposition and changes into heavy oil (100,101) by processes such as water washing (102). When the operating pressure of the separator is reduced, certain hydrocarbons with lower molecular weights (ranging from C_3 to C_6) in crude oil transition from the liquid phase to the vapor phase due to operational pressure, producing more gas and less oil (103). The oil produced, which exhibits a heavier oil phase characterized by limited solubility, high viscosity, and a larger density than water (104), presents significant challenges in the process of treatment. One challenge in treating crude oil is effectively removing the salt content from the heavy (high-density) oil phase. This is particularly difficult for heavier crudes, as they have more stable and complex emulsions that are harder to separate compared to lighter crudes.

Table 4.6 Effect of various first stage pressures on salt and water content concentration.

Pressure (barg)	Salt Outlet (PTB)	Water Content Outlet (Fraction)
64	5.775	0.0062
62	5.762	0.0062
60	5.749	0.0062
58	5.736	0.0062
56	5.722	0.0062
54	5.708	0.0062
52	5.693	0.0062
50	5.677	0.0062
48	5.661	0.0062
46	5.644	0.0062
44	5.625	0.0062
42	5.606	0.0062
40	5.585	0.0062
38	5.563	0.0062
36	5.539	0.0062
34	5.513	0.0062
32	5.485	0.0062
30	5.453	0.0062
28	5.417	0.0062
26	5.377	0.0062
24	5.330	0.0063
22	5.275	0.0063
20	5.209	0.0063
18	5.115	0.0063
16	4.986	0.0063
14	4.860	0.0062

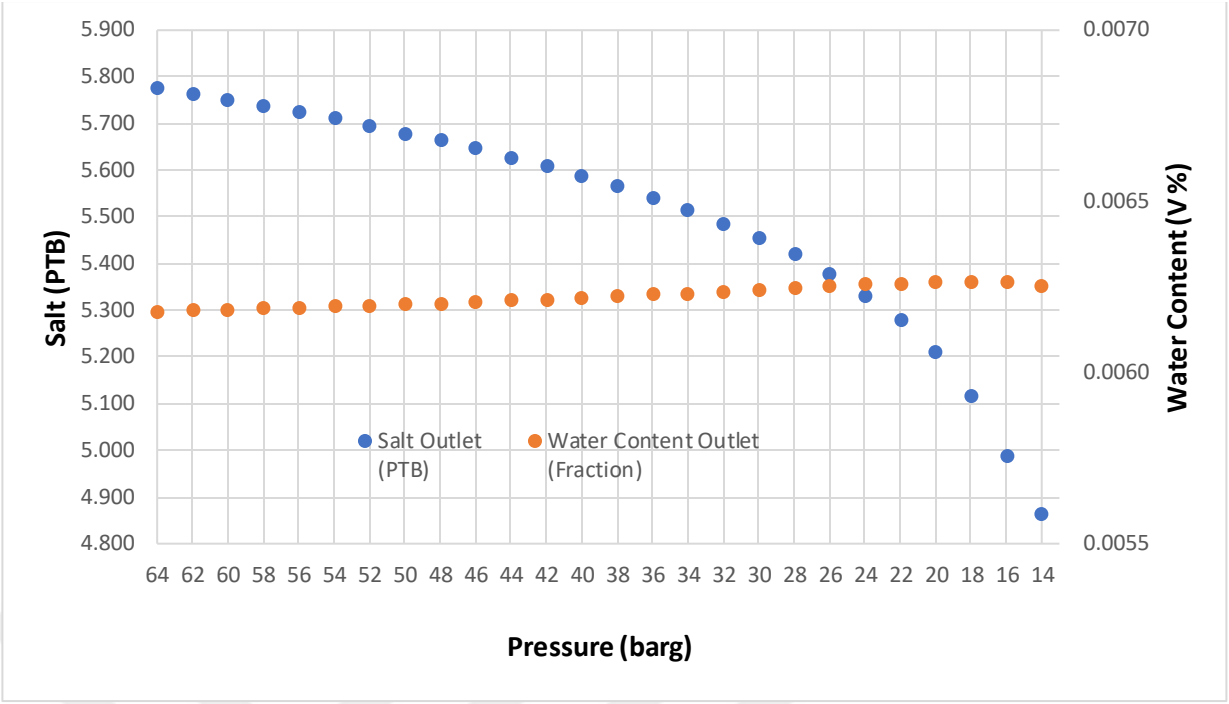

Figure 4.5 First stage pressure effect on salt concentration and water content.

4.3.3 Wash Water Flow Rate Effect

Crude oil train facilities demonstrate a wash water flow rate of 3154 bbl/day (nearly 21 m^3/h), which corresponds to 3% of the crude oil feed of the train. In the simulation conducted, the wash water was altered in increments of 250 bbl/day, ranging from 1000 to 6000 bbl/day, while keeping all other variables constant (crude oil inlet flow rate, pressure, and temperature). According to the findings depicted in **Figure 4.6** and the data provided in **Table 4.7**, increasing the proportion of wash water leads to a marginal reduction, from 51010 to 50985 bbl/day, in the flow rate of desalted oil (i.e., the proportional increase in effluent water corresponds to the marginal decrease in oil). This decrease is followed by a stable production of gas at 1.749 MMSCFH. Initially, the water present in the 1st and 2nd stage separators is being drained, resulting in improved water cut efficiency. However, this process also leads to the conveyance of salt crystals and crude oil to the subsequent stage, namely the dehydration stage. A greater amount of crystalline salt dissolves in the wash water as the flow rate increases, leading to a very slight (almost imperceptible) volumetric reduction in oil production. Modifying the flow rate of wash water does not increase the energy levels of hydrocarbon molecules in diluted crude oil. As a result, it is clear from **Figure 4.6** that there are no reversal

curves (parallel), which would indicate that gas and oil curves are not a function of wash water.

Table 4.7 Effect of various wash water ratios on oil and gas flow rates.

Wash Water (bbl/day)	Desalted Oil Flow Rate (bbl/day)	Gas Flow Rate (MMSCFH)
1000	51010	1.749
1250	51006	1.749
1500	51003	1.749
1750	51001	1.749
2000	51000	1.749
2250	50998	1.749
2500	50997	1.749
2750	50996	1.749
3000	50995	1.749
3250	50994	1.749
3500	50993	1.749
3750	50992	1.749
4000	50991	1.749
4250	50990	1.749
4500	50990	1.749
4750	50989	1.749
5000	50988	1.749
5250	50987	1.749
5500	50987	1.749
5750	50986	1.749
6000	50985	1.749

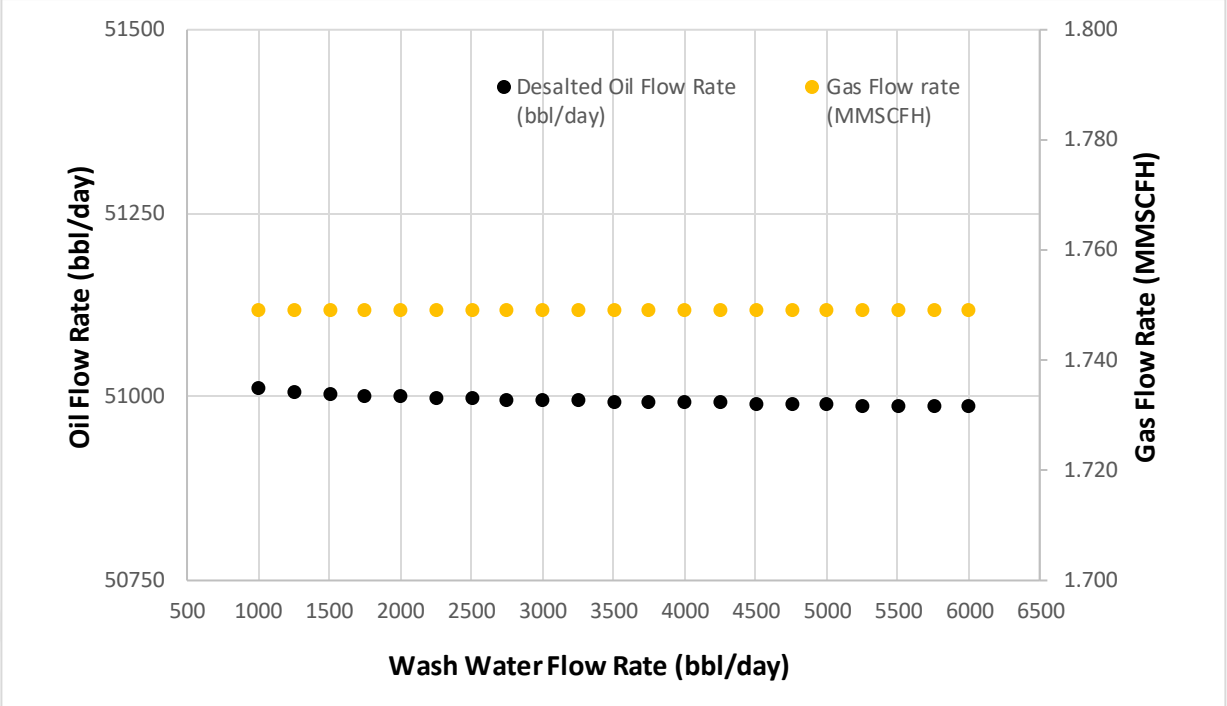

Figure 4.6 Wash water effect on oil and gas flow rates.

It can be noted that the salt concentration decreases from 30.808 to 1.500 PTB (95% reduction) in response to variations in the flow rate of wash water. Due to the enhanced flow rate of the wash water, a greater quantity of crystalline salt in crude oil undergoes dissolution in the wash water, producing desalted oil and salty water to be drained. The water content of the desalted oil remains constant regardless of changes in the flow rate of wash water, as shown in **Figure 4.7** and **Table 4.8**. This finding implies that the presence of wash water does not have an impact on the water content of the oil produced during the separation process of crude oil. The separator efficiently eliminates any excess water present in the associated water, leading to a consistent water content fraction of 0.0062 in the oil at the exit. In spite of this, it is important to note that too much wash water flow rate does affect negatively the process of crude oil train (i.e., excessive wash water through PDVs causes emulsion formation). At a wash water flow rate of 3%, the effectiveness of salt removal surpasses the efficiency of water separation and continues to increase as the wash water rate increases. In a related context, the efficiency of the water cut exhibited a decline as the rate of washing water rose.

Table 4.8 Effect of various wash water ratios on salt and water content concentration.

Wash Water (bbl/day)	Salt in Oil Outlet (PTB)	Water Content in Oil Outlet (Fraction)
1000	30.808	0.0062
1250	22.380	0.0062
1500	16.959	0.0063
1750	13.335	0.0063
2000	10.706	0.0063
2250	8.780	0.0063
2500	7.329	0.0063
2750	6.209	0.0063
3000	5.326	0.0063
3250	4.619	0.0062
3500	4.044	0.0062
3750	3.570	0.0062
4000	3.174	0.0062
4250	2.841	0.0062
4500	2.569	0.0062
4750	2.325	0.0062
5000	2.113	0.0062
5250	1.928	0.0062
5500	1.767	0.0062
5750	1.625	0.0062
6000	1.500	0.0062

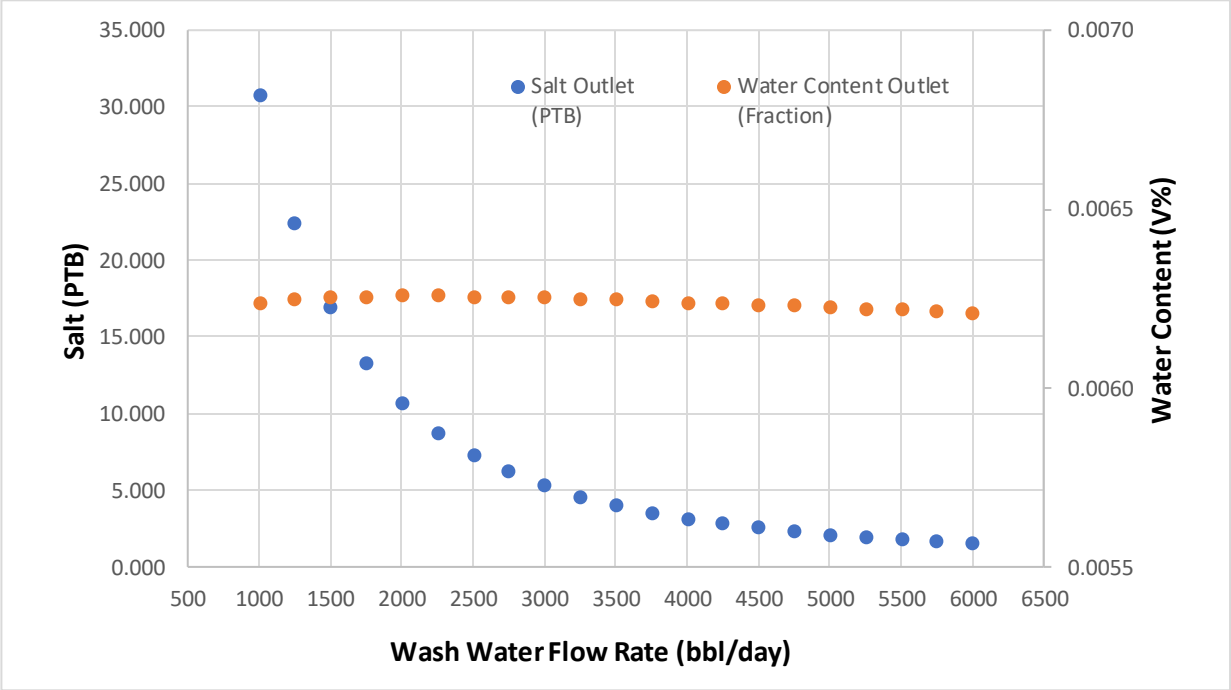

Figure 4.7 Wash water effect on salt concentration and water content.

4.3.4 Crude Oil Feed Rate Effect

Typically, the crude oil treatment plant operates at a flow rate of 116834 bbl/day. The conducted simulation varies the inlet's flow rate in increments of 10,000 bbl/day, with a flow range of 50,000 to 200,000 bbl/day. This variation is implemented while maintaining all other variables at a constant level, including pressure, temperature, and the flow rate of wash water. The simulated case study shows that changing the amount of crude oil feed from 50,000 to 200,000 bbl/day increases the flow rate of desalted oil from 22765 to 91061 bbl/day in a consistent way. Processively, this modification ensures a progressive increase in the rate of gas flow, ranging from 0.781 to 3.123 MMSCFH, as shown in **Figure 4.8** and the data presented in **Table 4.9**.

It's important to mention that R^2 of the desalted oil flow rate and gas flow rate regarding the feed variable are 1.0 and 1.0, respectively.

Table 4.9 Effect of various crude oil flows on oil and gas flow rates.

Crude Oil Inlet Flow Rate (bbl/day)	Desalted Oil Flow Rate (bbl/day)	Gas Flow Rate (MMSCFH)
50000	22765	0.781
60000	27318	0.937
70000	31871	1.093
80000	36424	1.249
90000	40977	1.405
100000	45531	1.562
110000	50084	1.718
120000	54637	1.874
130000	59190	2.030
140000	63743	2.186
150000	68296	2.342
160000	72849	2.498
170000	77402	2.655
180000	81955	2.811
190000	86508	2.967
200000	91061	3.123

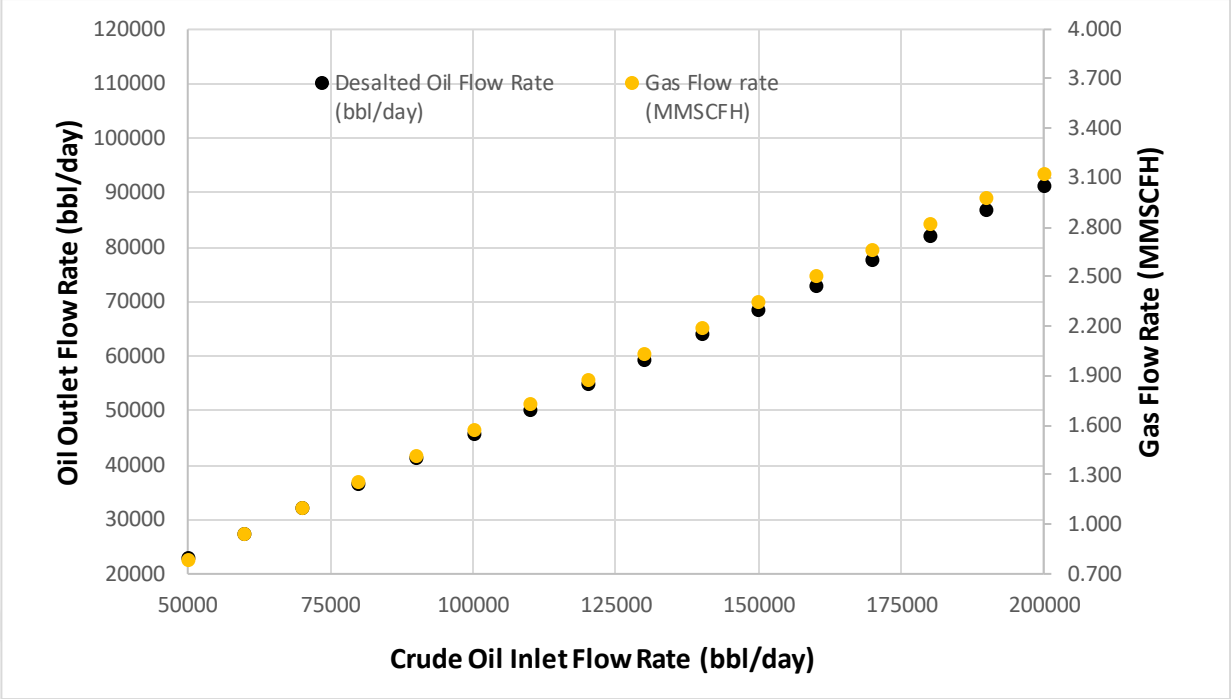

Figure 4.8 Crude oil inlet effect on oil and gas flow rates.

The simulation results indicate that there is not a significant relationship between variations in the crude oil inlet flow rate, and the concentration of salts found in processed oil. The observations indicated a consistent salt concentration ranging from 4.869 to 4.871 PTB in the correlation with variations in the crude oil input feed. The water content of the desalted oil remains constant regardless of variations in the feed flow rate (0.0062) due to the control equipment (interface level) of the crude oil train, as depicted in **Figure 4.9** and **Table 4.10**.

Table 4.10 Effect of various crude oil rates on salt and water content concentration.

Crude Oil Inlet Flow Rate (bbl/day)	Salt Outlet (PTB)	Water Content Outlet (Fraction)
50000	4.869	0.0063
60000	4.879	0.0063
70000	4.878	0.0063
80000	4.876	0.0063
90000	4.875	0.0063
100000	4.875	0.0063
110000	4.874	0.0063
120000	4.873	0.0062
130000	4.873	0.0062

Table 4.10 Continued.

140000	4.872	0.0062
150000	4.872	0.0062
160000	4.872	0.0062
170000	4.871	0.0062
180000	4.871	0.0062
190000	4.871	0.0062
200000	4.871	0.0062

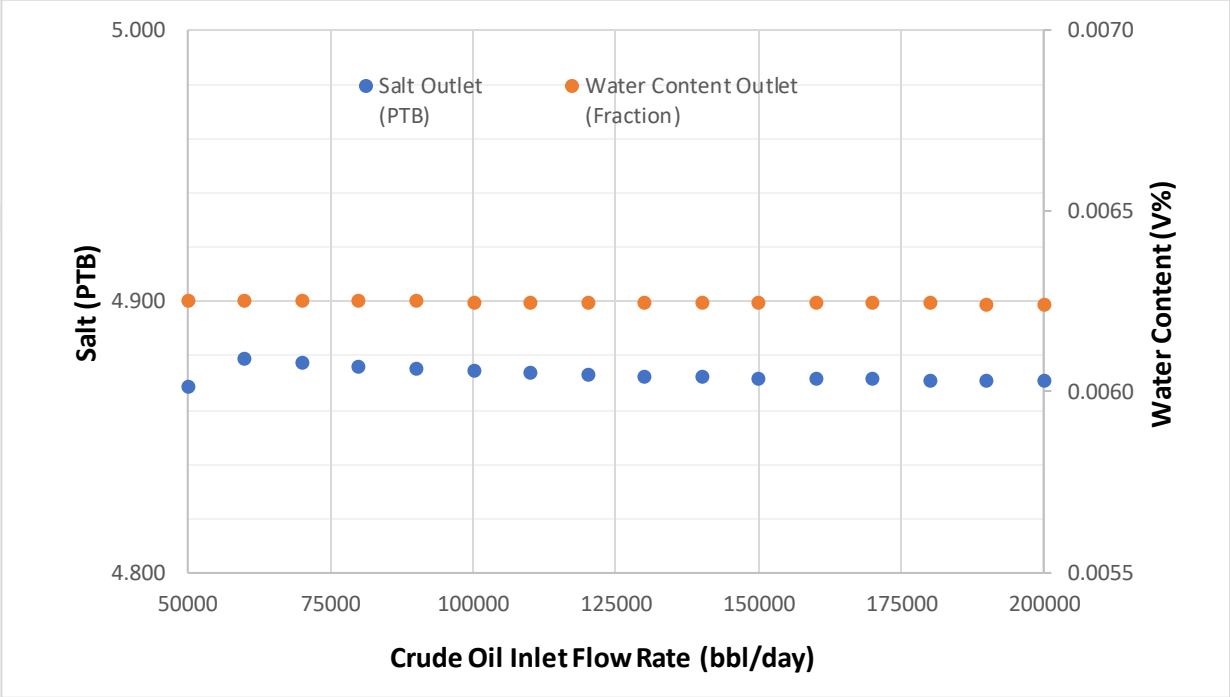

Figure 4.9 Crude oil inlet effect on salt concentration and water content.

4.3.5 Demulsifier Dosing Effect

Natural surfactants and resins of crude oil stabilize water-oil emulsions, which require demulsifiers to break down their high stability. Given the high cost of chemical demulsifiers, which typically range from 1.5 to 2.8 dollars per kilogram (105), or about 1.4 to 2.6 dollars per liter (the density of the EPT-# demulsifier is equal to 0.95 g/ml), it's crucial to address the issue of minimizing their usage as much as possible.

For that, the comparison of the simulation salt content between the field case and the improved scenario (case 3) shows how changing the operational parameters can greatly improve the feasibility of the process overall. The bottle test approach is employed to evaluate the impact of EPT-# doses on improved crude oil samples

(i.e., samples used in this test have conditions like case 3), with concentrations ranging from 0 to 30 ppm as follows: tube no. 1 = 10 ppm, tube no. 2 = 13 ppm, tube no. 3 = 16 ppm, tube no. 4 = 19 ppm, tube no. 5 = 25 ppm, tube no. 6 = 30 ppm, and tube no. 7 = 0 ppm (blank).

As shown in **Figure 4.10**, the test result of the bottles recorded as a percentage of water separated from the samples after 20 minutes was as follows: tube no. 1 = 22%, tube no. 2 = 26%, tube no. 3 = 42%, tube no. 4 = 42%, tube no. 5 = 42%, tube no. 6 = 42%, and tube no. 7 = 0%.

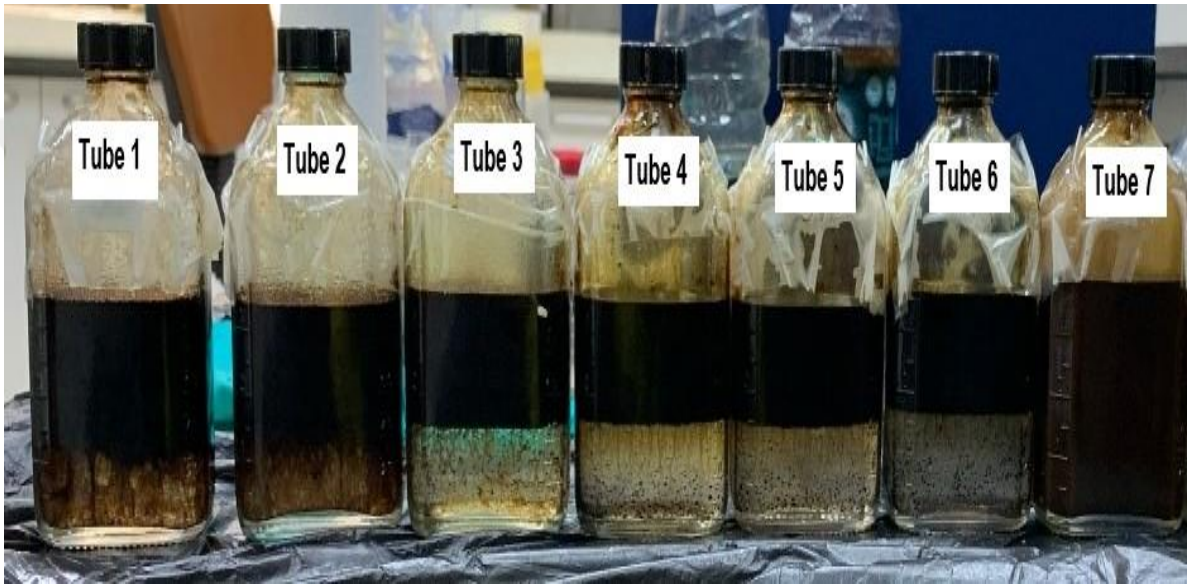

Figure 4.10 The bottle test shows different separated water levels.

The results above indicated that tube No. 3 exhibited the highest accepted level of water separation (42%), with a lower dosage of demulsifier (16 ppm). Although the percentage of water separated in tubes No. 4, 5, and 6 was equal to that in tube No. 3, their dosages were over at 19, 25, and 30 ppm, respectively. While tubes No. 1 and 2 show less separated water (22% for tube No. 1 and 26% for tube No. 2), due to the lower dosage (i.e., not enough demulsifier to breakdown the emulsion), it's important to mention that tube No. 7 does not get any water separation due to a nil dosage of demulsifier.

This procedure reduces the demulsifier's consumption dosage, whereas in real-field applications, oil trains use the chemical demulsifier EPT-# at a concentration of 29 ppm (538 L/day). Under the improved conditions of this study,

an effective dosage at a concentration of 16 ppm (297 L/day) means reducing the operating expenses of the demulsifier by 45% (241 L/day).

For the scope of this work, the savings in operating costs related to chemical demulsifiers would be in the order of 0.004 dollars per barrel of oil produced (the demulsifier average price chosen is 2 dollars per liter). In order to assess the viability of reducing demulsifier expenses, it's important to consider a huge oil-producing country like Iraq, which exports over 3.4 million barrels of oil per day (Iraq's 2023 oil exports surpassed 1.2 billion barrels). Accordingly, reflecting the result above (0.004 $/bbl) on overall produced crude oil may lead to savings in the order of 5 million $/year.

4.4 Case Study

This part of the thesis presents the findings of a deeper simulation investigation that examined the impact of enhancing desalting operational parameters, such as temperature, pressure, wash water flow, and chemical demulsifier dose, on a crude oil train located in a specific field in Basra, southern Iraq. The improvement of the process involves several steps. Firstly, simulate the normal operation conditions of the crude oil train, which is case 1 (i.e., real data from plant field input in the HYSYS simulation), then the temperature and pressure of the crude oil train, which is case 2, are determined due to the reduced salt concentration from 4.86 PTB (case 1) to 3.02 PTB (case 2). Second, decreasing the wash water flow rate in case 2 gradually until the salt concentration returns to its original level in the normal conditions of case 1 (i.e., until the salt concentration is back to 4.86 PTB). It’s important to mention that the flow rate of wash water decreased from 21 m^3/h (case 2) to 16 m^3/h (case 3). Finally, compare the actual salt concentration of the field plant with the improved case to determine the ideal dosage of the chemical demulsifier.

4.4.1 Phase Envelope Analysis (P-T Envelope)

The phase envelope is a valuable tool for identifying improved operating conditions by displaying the pressure and temperature values at which a system can exist in either a single phase or two phases. This information is crucial for facilitating efficient design processes. It is crucial to comprehend that separators functioning beyond the dew point line under constant pressure and elevated temperature conditions lead to the total transfer of the constituents of the oil phase into the gas phase. Conversely, in the event that the operating conditions were

beyond the bubble point curve at a consistent temperature, only the oil phase would be present. Hence, it can be concluded that the separator's improved operating parameters were inside the two-phase region, ensuring the highest possible recovery of both gas and oil.

The gas stream phase envelope from the HYSYS simulation under the field conditions depicted in **Figure 4.11**, illustrates that the specific operating parameters of the gas outlet stream were 53.5 °C and 33.1 barg, which lie in the two-phase region and are far from the dew point curve (i.e., gas not recovered completely from crude oil). So, it's important to induce a transition in phase from a mixture of gas and oil to the gas phase only. Improvement of the process parameters by an alteration of temperature from 50 °C to 80 °C and pressure from 41.5 barg to 14 barg was simulated. The gas stream phase envelope of the new parameters (80 °C and 14 barg), as shown in **Figure 4.12**, clarifies that the specific operating parameters of the gas outlet stream were 79.5 °C and 4.8 barg lie on the dew point curve (i.e., the stream of gas phase), and this transition of phase would result in a concomitant modification in the rate of gas flow from 1.749 to 1.953 MMSCFH. HYSYS produces a gas stream with a cricondentherm of 101.8 °C at a pressure of 50.15 barg.

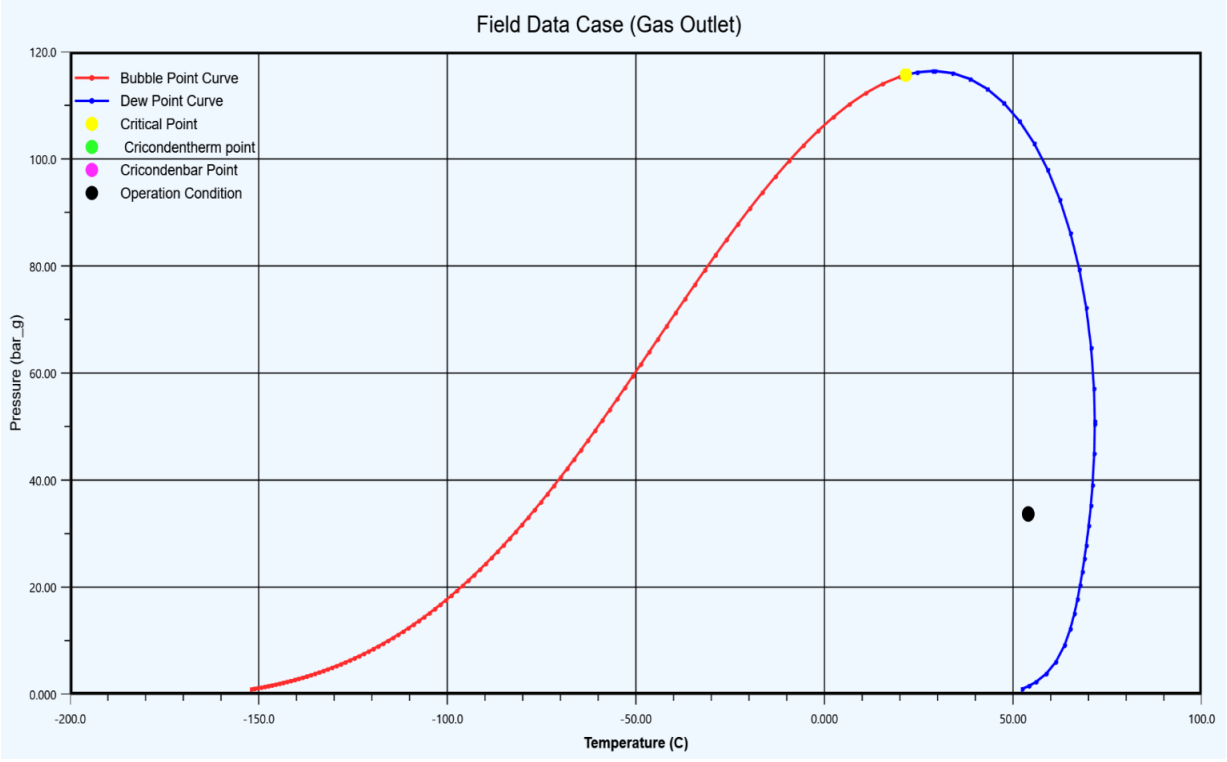

Figure 4.11 Phase envelope of gas outlet (Field Case).

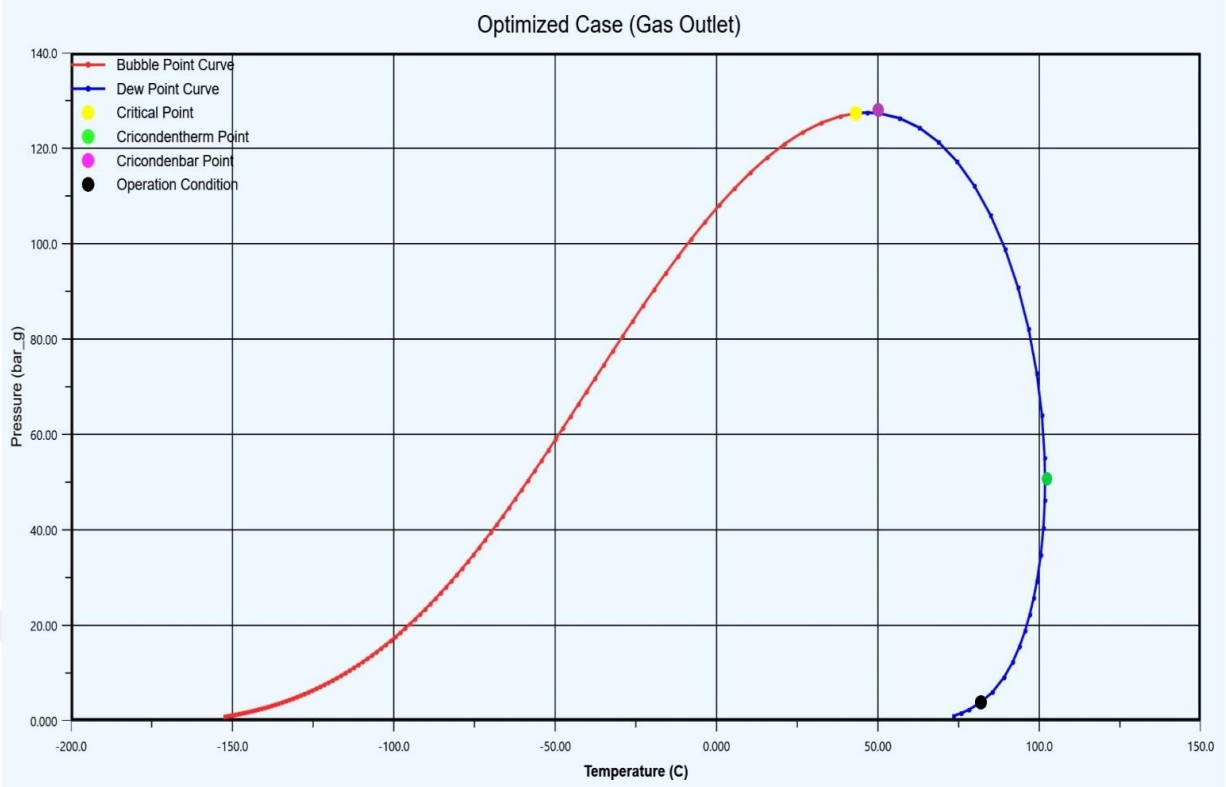

Figure 4.12 Phase envelope of gas outlet (Improved Case).

Based on the phase envelope of the oil outlet shown in **Figure 4.13**, it's evident that the operational condition of the outlet oil at 83.2 °C and 5.6 barg lies beyond the bubble point curve (i.e., subcooled oil). Therefore, it can be deduced that changes in either pressure or temperature would trigger a phase transition, which would then impact the oil production rate. Observing the given cricondenbar (35.91 barg at 525.7 °C) reveals that temperature changes do not affect the oil production rate. Additionally, it provides insight into potential methods for further refining the oil phase. In the context of a medium-pressure separator, it is crucial to carefully determine both pressure and temperature parameters to ensure that the oil phase maintains the appropriate stability level, whether it is directed towards a low-pressure separator or a storage tank that typically operates under atmospheric circumstances.

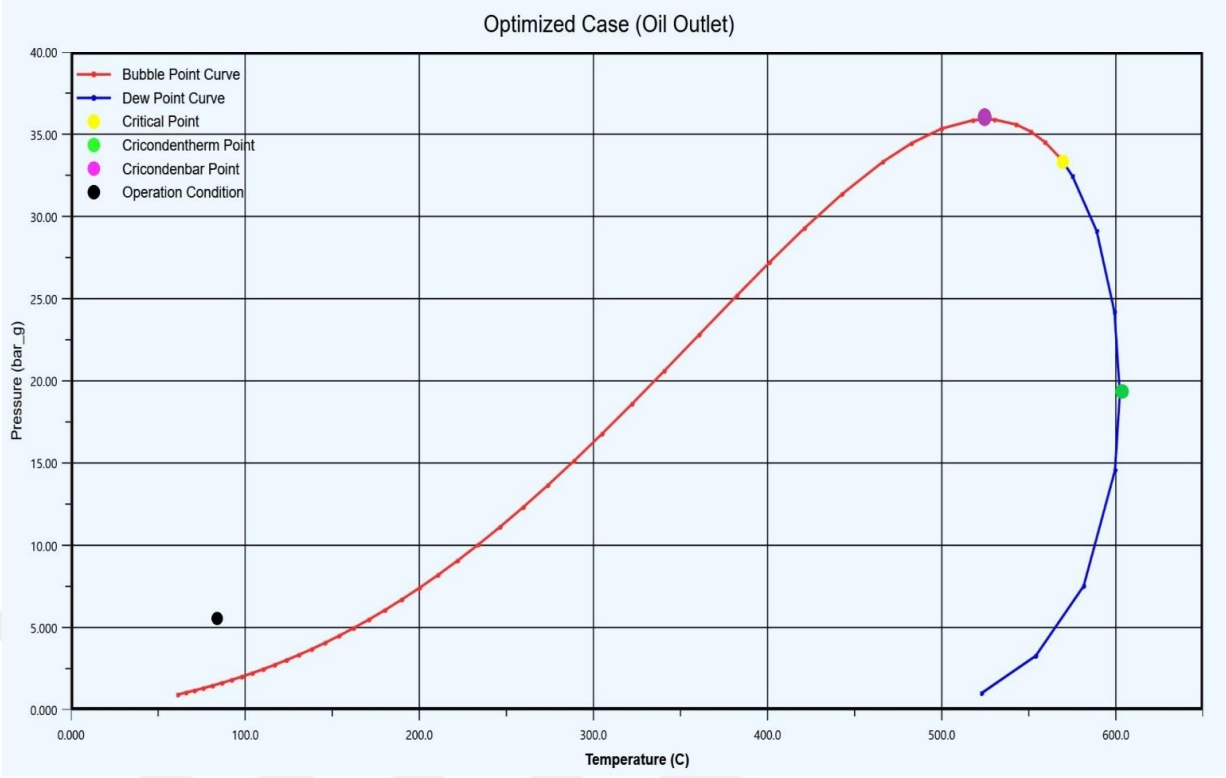

Figure 4.13 Phase envelope of oil outlet (Improved Case).

The successful separation of the hydrocarbon mixture is lead to the efficient recovery of condensate from the mixture. Therefore, it is feasible to obtain both qualitative and quantitative outcomes through the measurement of parameters such as gas-oil ratio (GOR), oil formation volume factor (Bo), and API density of crude oil (106). The ideal temperature and pressure settings, as shown in **Appendix 2: Process Flow Diagram for Simulation Case 2**, leads to a decrease in the salt content from 4.860 PTB (case 1) to 3.028 PTB (case 2).

4.4.2 Wash Water Rate Consumption Improvement

In relation to the topic of wash water conservation, the Case 3 simulation process achieved a significant decrease in the consumption of wash water for the purpose of crude oil washing by over 120 m^3/day (24% less in comparison to Case 1). The simulation process achieves this reduction while maintaining a salt content close to the field-case result of 4.9 PTB. The simulations show that the flow rate of wash water drops from 21 m^3/h (case 1) to 16 m^3/h (case 3). **Appendix 3: Process Flow Diagram for Simulation Case 3**, which represents the flow sheet based on which the results have been calculated by Aspen HYSYS, shows the best

(improved) flow rate of wash water under the improved temperature and pressure conditions.

For more detailed information on the design and operation parameters of all crude oil simulation cases, as well as a comparison of key results, see **Appendix 4: Equipment design parameters of train simulation** and **Appendix 5: Operation parameters and the key results of simulation**.

5. CONCLUSIONS AND RECOMMENDATIONS

The thesis's scope was to improve the crude oil desalting process using validated flowsheet simulation. We used the simulation to figure out the most effective formula for parameters of the crude oil treatment train that impact the desalting process by analyzing real-data of crude oil samples gathered from one of the Basra oil fields in the south of Iraq. Wherase Aspen HYSYS software was employed to construct the simulation of a crude oil train based on the analysis data of crude oil samples and the operational parameters of a flowsheet-validated in the field.

The HYSYS-based flowsheet simulation looked at how factors like temperature, pressure, wash water rate, feed flow, and demulsifier dose affected the amount of salt in the produced oil. Case studies of the Aspen HYSYS simulation were used to investigate the primary parameters that affect the operation of the crude oil desalting train. The operation conditions of the field train (case 1) include a temperature of 50 °C, a pressure of 41.5 barg, a wash water flow rate of 21 m^3, a crude oil feed of 116834 bbl/day, and a demulsifier dosage of 29 ppm.

An improved model of the crude oil train was built by determining the ideal level of separation among the studied parameter ranges and analyzing crude oil desalting by Aspen HYSYS simulation. The improved predictive conditions for crude oil treatment (case 3) are as follows: a temperature of 80 °C, a pressure of 14 barg, a wash water flow rate of 16 m^3, a crude feed rate of 116834 bbl/day, and a demulsifier dosage of 16 ppm. This model, in turn, has a significant impact on the desalting process as well as the overall feasibility of the crude oil train.

The simulation process resulted in a significant reduction in the use of wash water for crude oil washing. The decrease was accomplished while maintaining the desired crude oil quality, notably by ensuring that the salt concentration remained within the allowed range of 4.9 PTB. The simulations demonstrated a decrease in the flow rate of wash water from 21 m^3/h to 16 m^3/h (i.e., a reduction of 24%).

According to the data analysis, the field plant controller overestimates the condition, resulting in an excessive demulsifier injection rate that exceeds the necessary specification. The results of the bottle test of EPT-# doses on improved crude oil samples showed a reduction in operating expenses by implementing a decrease in chemical demulsifier (EPT-#) dosage from 29 ppm to 16 ppm, which is

a mean 45% drop in the total demulsifier used. The operating cost savings regarding the chemical demulsifiers would be in the range of 0.004 $/bbl of oil produced. This led to an improvement in overall separation efficiency and outcomes.

Maintaining an optimal level of performance presents a significant challenge. Consequently, it is crucial to prioritize monitoring efforts that have advisory elements, which provide guidance on how to address any deviations from the predetermined target. In general, this study effectively achieved the objective of keeping to the facility's specified standards for wash water conservation and salt concentration while simultaneously reducing chemical operating expenses.

For future work, it is critical to conduct multiple simulations by altering the dosage of demulsifier and the flow rate of fresh water while keeping the remaining variables unchanged. Collect the resulting data and analyze it with a model. It would be beneficial to determine if reduced demulsifier usage results in decreased fresh water consumption in the desalter, leading to substantial cost savings.

Given the limitations of HYSYS in simulating demulsifier processes, it is intriguing in the future to explore more sophisticated simulation tools for modeling the demulsification operation, like Materials Studio, GROMACS, and Neural Network Analysis. Additionally, it’s important to take into consideration that in the current modeling approach, we assumed that the associated water of crude oil would be pure water (i.e., the associated water of crude oil has impurities that were neglected because there is no way to simulate them). However, this assumption makes it hard to predict the stream features of the desalting process with high precision unless a tool can simulate these impurities, and this is another aspect that has potential for enhancement in the future of the simulation of the desalting process.

6. REFERENCES

"Vancouver citation system was used in this thesis."

1. Vafajoo L, Ganjian K, Fattahi M. Influence of key parameters on crude oil desalting: An experimental and theoretical study. J Pet Sci Eng. 2012;90–91:107–11.
2. Pereira J, Velasquez I, Blanco R, Sanchez M, Pernalete C, Canelón C. Crude Oil Desalting Process. Adv Petrochemicals. 2015;
3. Simanzhenkov V, Idem R. Crude Oil Chemistry. Crude Oil Chemistry. 2003.
4. Bratakh M, Toporov V, Romanova V. Crude Oil Processing. 2013. 125 p.
5. Abdel-Aal HK, Aggour MA, Fahim MA. Petroleum and Gas Field Processing. New York: CRC Press; 2003. 364 p. (Chemical Industries).
6. Selley RC, Sonnenberg SA. The Physical and Chemical Properties of Petroleum. In: Elements of Petroleum Geology. Elsevier; 2023. p. 15–42.
7. Levorsen AI. Geology of Petroleum. USA: American Association of Petroleum Geologists; 1967.
8. Hodgson GW. Vanadium, Nickel, and Iron Trace Metals in Crude Oils of Western Canada. Am Assoc Pet Geol Bull. 1954;38(12):2537–54.
9. Kimray. Types of Crude Oil: Heavy vs Light, Sweet vs Sour, and TAN count [Internet]. [cited 2023 Mar 25]. Available from: https://kimray.com/training/types-crude-oil-heavy-vs-light-sweet-vs-sour-and-tan-count
10. Coker AK. Petroleum Refining Design and Applications Handbook. Petroleum Refining Design and Applications Handbook. 2018.
11. EIA [Internet]. 2015 [cited 2023 Jul 16]. Under sanctions, Iran's crude oil exports have nearly halved in three years. Available from: http://www.bunkerportsnews.com/News.aspx?ElementId=386221cd-02fe-4791-b45b-daa0c4fbe3e9
12. Taheri SR, Pak A. Casing Failure in Salt Rock: Numerical Investigation of its Causes. Rock Mech Rock Eng. 2020;53(9):3903–18.
13. Speight JG. The Chemistry and Technology of Petroleum. 4th ed. The Chemistry and Technology of Petroleum. CRC Press; 2006. 984 p.
14. Gray MR, Eaton PE, Le T. Inhibition and promotion of hydrolysis of chloride salts in model crude oil and heavy oil. Pet Sci Technol. 2008;26(16):1934–44.
15. Sellami M, Naam R, Temmar M. Optimization of Operating Parameters of Oil Desalting in Southern Treatment Unit (HMD/Algeria). J Pet Environ Biotechnol. 2016;07(02).
16. Askari M, Aliofkhazraei M, Afroukhteh S. A comprehensive review on internal corrosion and cracking of oil and gas pipelines. J Nat Gas Sci Eng. 2019;71:102971.
17. Parker HD, Pitt GD. A technical review of the principles of oil-water separation. Pollut Control Instrum Oil Effluents. 1987;175–94.
18. Ditria JC, Hoyack ME. The Separation of Solids and Liquids With Hydrocyclone-Based Technology for Water Treatment and Crude Processing. In: All Days. SPE; 1994.
19. Rosso F, Sona G. Gravity-driven separation of oil-water dispersions. Adv Math Sci Appl. 2001;11(1):127–51.

20. Sayda AF, Taylor JH. Modeling and control of three-phase gravity separators in oil production facilities. Proc Am Control Conf. 2007;4847–53.

21. Jaworski AJ, Meng G. On-line measurement of separation dynamics in primary gas/oil/water separators: Challenges and technical solutions-A review. J Pet Sci Eng. 2009;68(1–2):47–59.

22. Sjöblom J. Emulsions and Emulsion Stability. Second Edi. Vol. 132, Surfactant Science Series. CRC Press Taylor & Francis Group 2006; 1996. 662 p.

23. Jones TJ, Neustadter EL, Whittingham KP. Water-in-Crude Oil Emulsion Stability and Emulsion Destabilization By Chemical Demulsifiers. J Can Pet Technol. 1978;17(2):100–8.

24. Eley DD, Hey MJ, Lee MA. Rheological studies of asphaltene films adsorbed at the oil/water interface. Colloids and Surfaces. 1987;24(2–3):173–82.

25. Mohammed RA, Bailey AI, Luckham PF, Taylor SE. Dewatering of crude oil emulsions 3. Emulsion resolution by chemical means. Colloids Surfaces A Physicochem Eng Asp. 1994;83(3):261–71.

26. Yazdanmehr F, Nistor I. Demulsifier Selection for Water Separation From Heavy Crude Oil Emulsions of Iranian Oil Field. Rom J Pet Gas Technol. 2021;2(73)(1):62–72.

27. Bessler DU, Chilingarian G V. Chemical resolution of petroleum emulsions. Dev Pet Sci. 1987;19(PA):125–47.

28. Al-Otaibi M, Elkamel A, Al-Sahhaf T, Ahmed AS. Experimental investigation of crude oil desalting and dehydration. Chem Eng Commun. 2003;190(1):65–82.

29. Thayee Al-Janabi OY, Ibrahim MS, Waheed IF, Sayda AW, Spearman P. Breaking water-in-oil emulsion of Northern Iraq's crude oil using commercial polymers and surfactants. Polym Polym Compos. 2020;28(3):187–98.

30. Hadi HA, Mohammed TJ. Improvement in demulsification of Iraqi crude oil with water removal demulsifiers in oil fields. IOP Conf Ser Mater Sci Eng. 2020;737(1).

31. He M, Pu W, Wu T, Yang X, Li X, Liu R, et al. Investigation on the mechanism of heating effect influencing emulsifying ability of crude oil: Experimental and molecular dynamics simulation. Colloids Surfaces A Physicochem Eng Asp. 2023;671(April):131654.

32. Ishiyama EM, Heins A V., Paterson WR, Spinelli L, Wilson DI. Scheduling cleaning in a crude oil preheat train subject to fouling: Incorporating desalter control. Appl Therm Eng. 2010;30(13):1852–62.

33. Al-Kandari J. Desalting Crude Oil. J Kuwaiti Eng Issued by Kuwait Soc Eng. 1997;55:22–5.

34. Ahmadi S, Khormali A, Meerovich Khoutoriansky F. Optimization of the demulsification of water-in-heavy crude oil emulsions using response surface methodology. Fuel. 2022;323(January):124270.

35. Tauscher W. Static mixing and reaction technology. Chem Pet Eng. 1996 May 23;32(3):224–37.

36. Agar G. Agar's solution to desalting systems. 2000;

37. Strassner JE. Effect of pH on Interfacial Films and Stability of Crude Oil-Water Emulsions. J Pet Technol. 1968;20(03):303–12.

38. Kokal S. Crude-Oil Emulsions: A State-Of-The-Art Review. SPE Prod Facil. 2005 Feb 15;20(01):5–13.

39. Elgibaly AA, Nashawi IS, Tantawy MA, Elkamel A. FLOW PROPERTIES OF WEATHERED CRUDE OILS AND THEIR EMULSIONS. J Dispers Sci Technol. 1999 Apr;20(3):857–82.

40. Frising T, Noïk C, Dalmazzone C. The liquid/liquid sedimentation process: From droplet coalescence to technologically enhanced water/oil emulsion gravity separators: A review. J Dispers Sci Technol. 2006;27(7):1035–57.

41. Raya SA, Mohd Saaid I, Abbas Ahmed A, Abubakar Umar A. A critical review of development and demulsification mechanisms of crude oil emulsion in the petroleum industry. J Pet Explor Prod Technol. 2020;10(4):1711–28.

42. Hajivand P, Vaziri A. Optimization of demulsifier formulation for separation of water from crude oil emulsions. Brazilian J Chem Eng. 2015;32(1):107–18.

43. Chawla ML. Field Desalting of Wet Crude in Kuwait. Soc Pet Eng AIME, SPE. 1987;165–75.

44. Taylor SE. Investigations into the electrical and coalescence behaviour of water-in-crude oil emulsions in high voltage gradients. Colloids and Surfaces. 1988;29(1):29–51.

45. Schramm LL. Petroleum Emulsions. In: Emulsions : fundamentals and applications in the petroleum industry. 1992. p. 1–49.

46. Karyappa RB, Thaokar RM. Electric-field-assisted formation of nonspherical microcapsules. Langmuir. 2014;30(34):10270–9.

47. Sjöblom J, Mhatre S, Simon S, Skartlien R, Sørland G. Emulsions in external electric fields. Adv Colloid Interface Sci. 2021;294(May).

48. Luo S, Schiffbauer J, Luo T. Effect of electric field non-uniformity on droplets coalescence. Phys Chem Chem Phys. 2016;18(43):29786–96.

49. Lucas RN. Dehydration of heavy crudes by electrical means. Soc Pet Eng - Fall Meet Soc Pet Eng AIME, FM 1966. 1966;

50. Lucas RN. Performance of Heavy Oil Dehydrators. J Pet Technol. 1969 Oct 1;21(10):1285–92.

51. Behin J, Aghajari M. Influence of water level on oil-water separation by residence time distribution curves investigations. Sep Purif Technol. 2008;64(1):48–55.

52. Check GR. Two-stage ultrasonic irradiation for dehydration and desalting of crude oil: A novel method. Chem Eng Process Process Intensif. 2014;81:72–8.

53. Nikkhah M, Tohidian T, Rahimpour MR, Jahanmiri A. Efficient demulsification of water-in-oil emulsion by a novel nano-titania modified chemical demulsifier. Chem Eng Res Des. 2015;94:164–72.

54. Farrokhi F, Jafari Nasr MR, Rahimpour MR, Arjmand M, Vaziri SA. Application of a novel magnetic nanoparticle as demulsifier for dewatering in crude oil emulsion. Sep Sci Technol. 2018;53(3):551–8.

55. Ibrahim RI, Odah MK, Salman HS. Pressure wave elimination in Iraqi crude oil pipelines using novel porous filter and electronic control system. Int J Eng Technol. 2018;7(4.7 Special Issue 7):106–15.

56. Basher NA, Abdulkhabeer A. Synthesis of novel demulsifier nano-materials and their application in the oil industry. Mater Today Proc. 2021;49(November):2842–50.

57. Wang J, Yu Z, Xiao X, Chen Z, Huang J, Liu Y. A novel hydroxyapatite super-hydrophilic membrane for efficient separation of oil-water emulsions, desalting and removal of metal ions. Desalination. 2023 Nov;565:116864.

58. Reed M, Gundlach E, Kana T. A coastal zone oil spill model: Development and sensitivity studies. Oil Chem Pollut. 1989;5(6):411–49.

59. Abdel-Aal HK, Redhwi HH. Crude Oil Treatment: Dehydration, Desalting, and Stabilization. Petroleum Economics and Engineering. CRC Press; 2013. 298–309 p.

60. Abdel Aal HK, Zohdy K, Abdelkreem M. Waste Management in Crude Oil Processing: Crude Oil Dehydration and Desalting. Int J Waste Resour. 2018;08(01):8–11.

61. Chang B, Lee S, Kwon H, Moon I. Rigorous industrial dynamic simulation of a crude distillation unit considered valve tray rating parameters. Comput Chem Eng. 1998;22(SUPPL.1):863–6.

62. Wang W, Watkinson AP. Iron sulphide and coke fouling from sour oils: Review and initial experiments. Proc Int Conf Heat Exch Fouling Clean IX. 2011;(June 2011):23–30.

63. Groysman A. Corrosion problems and solutions in oil, gas, refining and petrochemical industry. Koroze a Ochr Mater. 2017;61(3):100–17.

64. Alhajri I, Elsholkami M. Techno-economic assessment of heavy crude oil desalting plant. Int J Oil, Gas Coal Technol. 2014;8(3):275–90.

65. Zhang F, Zhang Q, Zhou Z, Sun L, Zhou Y. Study on the Effect of Different Viscosity Reducers on Viscosity Reduction and Emulsification with Daqing Crude Oil. Molecules. 2023;28(3):1–11.

66. Sun R, Shook CA. Inversion of heavy crude oil-in-brine emulsions. J Pet Sci Eng. 1996;14(3–4):169–82.

67. Faizullayev S, Adilbekova A, Kujawski W, Mirzaeian M. Recent demulsification methods of crude oil emulsions – Brief review. J Pet Sci Eng. 2022 Aug;215:110643.

68. Pekdemir T, Akay G, Dogru M, Merrells RE, Schleicher B. Demulsification of highly stable water-in-oil emulsions. Sep Sci Technol. 2003;38(5):1161–83.

69. Eow J. Electrostatic enhancement of coalescence of water droplets in oil: a review of the technology. Chem Eng J. 2002 Jan 28;85(2–3):357–68.

70. Aryafard E, Farsi M, Rahimpour MR. Modeling and simulation of crude oil desalting in an industrial plant considering mixing valve and electrostatic drum. Chem Eng Process Process Intensif. 2015;95:383–9.

71. Mahdavi S, Mousavi Moghadam A. Critical Review of Underlying Mechanisms of Interactions of Asphaltenes with Oil and Aqueous Phases in the Presence of Ions. Energy & Fuels. 2021 Dec 2;35(23):19211–47.

72. Abdulredha MM, Hussain SA, Abdullah LC, Hong TL. Water-in-oil emulsion stability and demulsification via surface-active compounds: A review. J Pet Sci Eng. 2022 Feb;209:109848.

73. Becher P. ed. Encyclopedia of Emulsion Technology. Marcel Dekker, New York. 1983;1:415.

74. Sjöblom J. Emulsions-A fundamental and practical approach. NATO ASI Ser ed Kluwert Acad Publ Dordr. 1992;

75. Dhuldhoya N, Mileo M, Faucher M, Sellman E. Dehydration of heavy crude oil using disc stack centrifuges. Proc - SPE Annu Tech Conf Exhib. 1998;1999-Septe:371–80.

76. Kim BY, Moon JH, Sung TH, Yang SM, Kim JD. Demulsification of water-in-crude oil emulsions by a continuous electrostatic dehydrator. Sep Sci Technol. 2002;37(6):1307–20.

77. Hosseinpour F, Ghader S, Rahimpour MR, Bagheri H. Modification of an Industrial Crude

Oil Desalting Unit By Electric Mixing To Improve the Dehydration Efficiency. J Chem Technol Metall. 2019;54(1):124–34.

78. Tahouni N, Abbasi M, Panjeshahi MH, Eddine MRN. Parametric optimization of a crude oil treatment unit to maximize oil production. Chem Eng Res Des. 2023;190:20–32.

79. Biglari M, Ilkhaani S, Alhajri I, Lohi A. Process design, simulation and integration of a new desalter in the crude distillation unit of a refinery. Int J Oil, Gas Coal Technol. 2010;3(4):350–61.

80. Rahmani M, Tahouni N, Abbasi M, Panjeshahi MH. Modeling and performance analysis of electrostatic desalter using combined CFD-PBM method. Chem Eng Res Des. 2023;194:121–35.

81. Fetter Pruneda E, Rivero E, Escobedo B, Javier F, Vázquez G. Optimum Temperature in the Electrostatic Desalting of Maya Crude Oil. J Mex Chem Soc. 2005;49(1):14–9.

82. Thro M, Arnold KE. Water droplet size determination for improved oil treater sizing. Proc - SPE Annu Tech Conf Exhib. 1994;Pi(pt 2):213–22.

83. Khalaf AH, Rajab MS. Crude Oil Desalting Using Multi-Surfactant Based on a Best Dosage, Solvent and Mixing Ratio. Tikrit J Eng Sci. 2019;26(2):23–7.

84. Akbarian Kakhki N, Farsi M, Rahimpour MR. Effect of current frequency on crude oil dehydration in an industrial electrostatic coalescer. J Taiwan Inst Chem Eng. 2016;67:1–10.

85. Eow JS, Ghadiri M, Sharif AO, Williams TJ. Electrostatic enhancement of coalescence of water droplets in oil: A review of the current understanding. Chem Eng J. 2001;84(3):173–92.

86. Eow JS, Ghadiri M, Sharif AO. Electrostatic and hydrodynamic separation of aqueous drops in a flowing viscous oil. Chem Eng Process Process Intensif. 2002 Sep;41(8):649–57.

87. Eow JS, Ghadiri M. Drop-drop coalescence in an electric field: The effects of applied electric field and electrode geometry. Colloids Surfaces A Physicochem Eng Asp. 2003;219(1–3):253–79.

88. Eow JS, Ghadiri M. The behaviour of a liquid-liquid interface and drop-interface coalescence under the influence of an electric field. Colloids Surfaces A Physicochem Eng Asp. 2003;215(1–3):101–23.

89. Lukyanets AS, Kavehpour HP. Effect of electric fields on the rest time of coalescing drops. Appl Phys Lett. 2008;93(19):2006–9.

90. Kavehpour HP. Coalescence of Drops. Annu Rev Fluid Mech. 2015 Jan 3;47(1):245–68.

91. Ibrahim DS, Sami NA. Experimental Study of Desalting and Dehydration of Two Samples of Iraqi Crude Oils. Pet Sci Technol. 2015;33(15–16):1533–9.

92. Kaal E, Janssen HG. Extending the molecular application range of gas chromatography. J Chromatogr A. 2008;1184(1–2):43–60.

93. Aspen Technology. Aspen Physical Property System 11 . 1. Aspen Technol Inc. 2001;(Property Method Descriptions):2–16.

94. Peng DY, Robinson DB. A New Two-Constant Equation of State. Ind Eng Chem Fundam. 1976;15(1):59–64.

95. Aspen Technology. Aspen Physical Property System: Physical Property Methods. Aspen Technol Inc. 2013;1–248.

96. Aspen Technology. Simulation Basis Guide. Aspen Technol Inc. 2011;1–558.

97. Price LC. Aqueous Solubility of Petroleum as Applied to Its Origin and Primary Migration. AAPG bulletin. 1976;60(2):213–44.

98. Price LC. Aqueous Solubility of Crude Oil To 400°C and 2,000 Bars Pressure in the Presence of Gas*. Vol. 4, Journal of Petroleum Geology. 1981. p. 195–223.

99. Noubigh A, Abderrabba M, Provost E. Temperature and salt addition effects on the solubility behaviour of some phenolic compounds in water. J Chem Thermodyn. 2007;39(2):297–303.

100. Bata T, Parnell J, Samaila NK, Abubakar MB, Maigari AS. Geochemical evidence for a Cretaceous oil sand (Bima oil sand) in the Chad Basin, Nigeria. J African Earth Sci. 2015;111:148–55.

101. Bata T, Parnell J, Bowden S, Boyce A. Origin of heavy oil in cretaceous petroleum reservoirs. Bull Can Pet Geol. 2016;64(2):106–18.

102. P. Bata T, Alexander Lar U, K. Samaila N, U. Dibal H, I. Daspan R, C. Isah L, et al. Effect of biodegradation and water washing on oil properties. AIMS Geosci. 2018;4(1):21–35.

103. Kokal S, Al-Ghamdi A. Performance appraisals of gas/oil-separation plants. SPE Prod Oper. 2008;23(2):287–96.

104. Llamas MR, Custodio E, editors. Intensive Use of Groundwater: Challenges and Opportunities. CRC Press; 2003. 118 p.

105. Nadirov KS, Sadyrbayeva AS, Moldabayeva GZ, Baibotayeva SE, Zeygman Y V. Reagent preparation for oil treatment and its use in the process of dehydration. J Ind Pollut Control. 2017;33(1):1075–84.

106. Olugbenga AG, Al-mhanna NM, Yahya MD, Afolabi EA, Ola MK. Three-Phase Separators Using Aspen Hysys. 2021;1–17.

7. APPENDICES

Appendix 1: Process Flow Diagram for Simulation Case 1

Note: Double-click on the process flow diagram below to open it as a pdf file for more resolution.

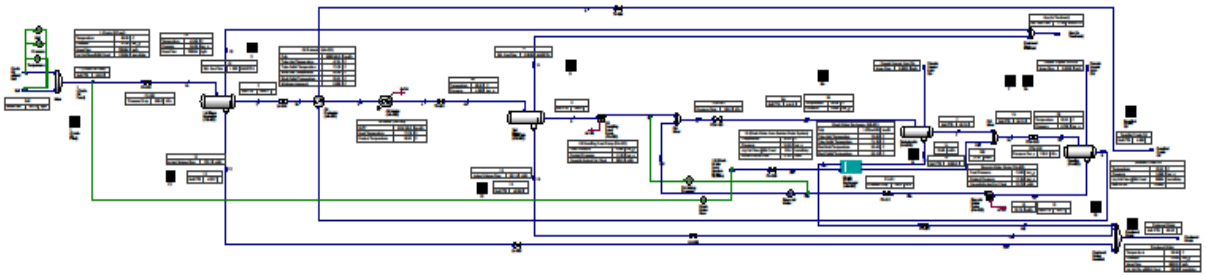

Appendix 2: Process Flow Diagram for Simulation Case 2

Note: Double-click on the process flow diagram below to open it as a pdf file for more resolution.

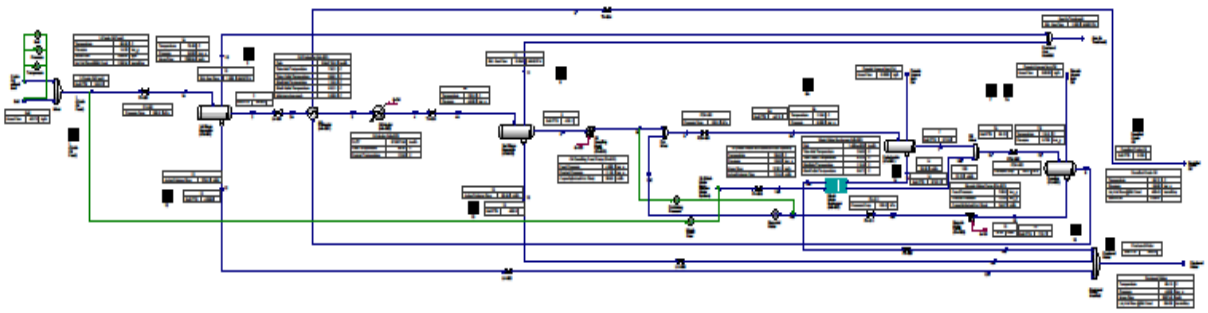

Appendix 3: Process Flow Diagram for Simulation Case 3

Note: Double-click on the process flow diagram below to open it as a pdf file for more resolution.

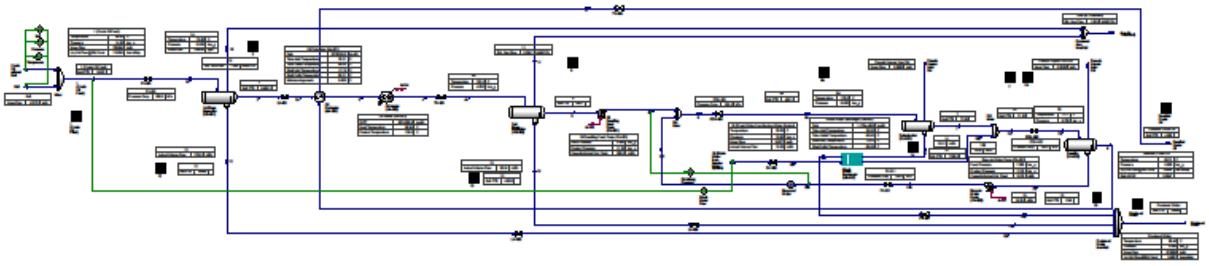

Appendix 4: Equipment design parameters of train simulation

Description	Value	Description	Value
1st Stage Separator (VS-001)		**2nd Stage Separator (VS-002)**	
Diameter (m)	3.6	Diameter (m)	3.1
Length (m)	17.5	Length (m)	15.0
Volume (m^3)	178.1	Volume (m^3)	113.2
Liq. Volume (%)	50	Liq. Volume (%)	50
Pressure (barg)	40.2	Pressure (barg)	7
Temperature (°C)	-5/+107	Temperature (°C)	-5 / +125
Dehydrator (VU-001)		**Desalter (VU-002)**	
Diameter (m)	3.0	Diameter (m)	3.0
Length (m)	11.8	Length (m)	11.8
Volume (m^3)	83.4	Volume (m^3)	83.4
Liq. Volume (%)	50	Liq. Volume (%)	50
Pressure (barg)	16	Pressure (barg)	16
Temperature (°C)	-5 / +125	Temperature (°C)	-5 / +125
Oil Pre-heater (HA-001)		**Oil Heater (HA-002)**	
Design Duty (Kcal/h)	6502000	Duty (Kcal/h)	9783000
Press. Shell Side (barg)	16	Press. Shell Side (barg)	26.7
Temp. Shell Side (°C)	125	Temp. Shell Side (°C)	260
Press. Tube Side (barg)	40.2	Press. Tube Side (barg)	40.2
Temp. Tube Side (°C)	116	Temp. Tube Side (°C)	125
Oil Desalting Feed Pump (PA-001)		**Recycle Water Pump (PA-002)**	
Flow Rate (m^3/h)	476	Flow Rate (m^3/h)	35.3
Delta P (kPa)	660	Delta P (kPa)	540
Wash Water Heat Exchanger (HB-001)		**FV-001**	

Design Duty (Kcal/h)	1594000	Delta P (kPa)	500
Press. Hot Side (barg)	16	**LV-001**	
Temp. Hot Side (°C)	125	Delta P (kPa)	0
Press. Cold Side (barg)	16	**TV-001**	
Temp. Cold Side (°C)	125	Delta P (kPa)	0
PDV-001		**PDV-002**	
Delta P (kPa)	155	Delta P (kPa)	100

Appendix 5: Operation parameters and the key results of simulation

Parameter	Case 1	Case 2	Case 3
Manifold			
Crude oil feed rate (bbl/day)	116834	116834	116834
Mass flow (kg/h)	706694	706694	706694
Pressure (barg)	41.5	14	14
Temperature (°C)	50	80	80
Salt content (PTB)	18192	18192	18192
1st Stage Separator (VS-001)			
Pressure (barg)	7.2	7.2	7.2
Temperature (°C)	47.6	78.2	78.2
Delta P (kPa)	2930	180	180
Gas Flow (MMSCFH)	1.663	1.859	1.859
Oil Flow (bbl/day)	62281	59643	59643
Water Flow (m^3/h)	270.1	278.8	278.8
Oil Salt (PTB)	8440	8468	8468
Water Salt (PTB)	40217	40399	40399
Oil Pre-heater (HA-001)			
Duty (Kcal/h)	6000245	5044725	5226108
Pressure Drop (kPa) Shell/Tube	140/140	140/140	140/140
Press. Shell Side (barg)	7.0	7.0	7.0
Temp. Shell Side (°C)	92.9	116.6	117.8
Press. Tube Side (barg)	7.2	7.2	7.2
Temp. Tube Side (°C)	47.6	78.2	78.2
Oil Heater (HA-002)			
Duty (Kcal/h)	6134195	5755778	5574395
Delta P (kPa)	100	100	100
Press. Tube Side (barg)	5.8	5.8	5.8

Temp. Tube Side (°C)	72.2	98.8	99.5
2nd Stage Separator (VS-002)			
Pressure (barg)	4.8	4.8	4.8
Temperature (°C)	95.6	120	120
Delta P (kPa)	0	0	0
Gas Flow (MMSCFH)	0.0855	0.0947	0.0947
Oil Flow (bbl/day)	51314	49343	49343
Water Flow (m^3/h)	88.14	85.54	85.54
Oil Salt (PTB)	406.5	409.1	409.1
Water Salt (PTB)	40383	40815	40815
Oil Desalting Feed Pump (PA-001)			
Flow Rate (m^3/h)	365.6	358.5	358.5
Delta P (kPa)	655	655	655
Dehydrator (VU-001)			
Pressure (barg)	9.7	9.7	9.7
Temperature (°C)	95.48	119.8	120
Delta P (kPa)	10	10	10
Gas Flow (MMSCFH)	0	0	0
Oil Flow (bbl/day)	51184	49207	49213
Water Flow (m^3/h)	23.86	25	19.51
Oil Salt (PTB)	60.28	57.09	72.95
Water Salt (PTB)	6089.6	5792.2	7396.5
Wash Water Heat Exchanger (HB-001)			
Duty (Kcal/h)	1079029	1498403	1179409
Press. Drop (kPa) Shell/Tube	100/100	100/100	100/100
Press. Hot Side (barg)	9.7	9.7	9.7
Temp. Hot Side (°C)	95.48	119.8	120
Press. Cold Side (barg)	9.9	9.9	9.9

Temp. Cold Side (°C)	25	25	25
Flow Rate Cold Side (m^3/h)	21.04	21.04	15.96
Flow Rate Hot Side (m^3/h)	23.86	25	19.51
Desalter (VU-002)			
Pressure (barg)	7	7	7
Temperature (°C)	92.98	116.6	117.8
Delta P (kPa)	170	170	170
Gas Flow (MMSCFH)	0	0	0
Oil Flow (bbl/day)	50994	48943	48946
Water Flow (m^3/h)	23.78	24.87	19.39
Oil Salt (PTB)	4.8	3.02	4.8
Water Salt (PTB)	842.1	770.7	1246
Recycle Water Pump (PA-002)			
Flow Rate (m^3/h)	23.78	24.87	19.39
Delta P (kPa)	535	535	535

Appendix 6: Critical properties of crude oil compositions

Composition	T_c (°C)	P_c (barg)	V_c (m^3/kgmol)	ω
H_2O	374.1	220.2	0.0571	0.3440
N_2	-147.0	32.93	0.0900	0.0400
CO_2	30.95	72.69	0.0939	0.2389
Methane	-82.45	45.39	0.0990	0.0115
Ethane	32.28	47.83	0.1480	0.0986
Propane	96.75	41.55	0.2000	0.1524
i-Butane	134.9	35.46	0.2630	0.1848
n-Butane	152.0	36.95	0.2550	0.2010
i-Pentane	187.2	32.32	0.3080	0.2220
n-Pentane	196.5	32.74	0.3110	0.2539
n-Hexane	234.7	29.30	0.3680	0.3007
C7*	271.1	29.40	0.3943	0.2854
C8*	299.9	27.44	0.4378	0.3176
C9*	328.3	25.48	0.4864	0.3541
C10-15*	405.9	20.18	0.6567	0.4802
C16-20*	493.6	14.97	0.9231	0.6697
C21-27*	558.7	12.06	1.155	0.8360
C28-35*	621.9	9.887	1.395	1.017
C36-47*	679.9	7.972	1.658	1.214
C48-80*	756.7	4.966	2.219	1.572
NaCl	651.9	62.99	0.1770	1.916